NPS ARCHIVE
1958
THURSTON, D.

AN EXPERIMENTAL INVESTIGATION OF FLAME SPREADING FROM BLUFF BODY FLAMEHOLDERS

DICK W. THURSTON

DUDLEY KNOX LIBRARY
NAVAL POSTGRADUATE SCHOOL
MONTEREY CA 93943-5101

AN EXPERIMENTAL INVESTIGATION OF FLAME SPREADING FROM BLUFF BODY FLAMEHOLDERS

Thesis by

Dick W. Thurston

Lieutenant, United States Navy

8854

In Partial Fulfillment of the Requirements

For the Degree of

Aeronautical Engineer

California Institute of Technology

Pasadena, California

1958

158
HURSTON, D.
467

ACKNOWLEDGEMENTS

I wish to express my sincere appreciation to Dr. E. E. Zukoski for suggesting the subject for investigation and for giving so freely of his time and knowledge in helping to carry this work to completion.

I am also deeply indebted to Dr. F. H. Wright, Senior Research Engineer at the Jet Propulsion Laboratory, for setting up the facilities used in this investigation and for his interest and day to day guidance during the progress of this work; to the laboratory personnel, and in particular to Mr. Carl Smith and Mr. Vernon Taylor for their patient efforts in maintaining and operating the equipment; to Mrs. Ingrid Stenberg who prepared the drawings, and to Mrs. Elizabeth Fox who typed the manuscript.

A special debt of gratitude is also due the Bureau of Aeronautics of the Navy Department which supported the entire three years of graduate study.

37653

ABSTRACT

Flame spreading from 1/16 to 1 inch circular cylinder flameholders in two-dimensional flow was studied experimentally. Combustion wake widths were determined by use of spark Schlieren photographs at distances up to 36 inches downstream of the flameholder in a 3 by 6 inch duct. The effect on wake width and flow parameters of several geometric and operating variables was observed.

The data show that above a critical approach gas velocity, corresponding to the transition from laminar to turbulent flow in the flame front, the wake width was independent of velocity and remained constant. Below the critical velocity the wake width was a strong function of velocity. Small but real effects were found on changing fuel-air ratios. The wake width was smallest and the wake spreading rate lowest at the stoichiometric fuel-air ratio. An eight to one variation in flameholder diameter resulted in only a 30 per cent variation in wake width at a distance of one duct height downstream. Farther downstream the variation was even less. Total and static pressure measurements showed that combustion processes fix the total pressure wake and that the losses associated with flameholder drag were not important in fixing the wake spreading rate.

TABLE OF CONTENTS

PART	TITLE	PAGE
	ACKNOWLEDGEMENTS	
	ABSTRACT	
	TABLE OF CONTENTS	
	LIST OF FIGURES	
	LIST OF SYMBOLS	
I	INTRODUCTION	1
II	EXPERIMENTAL APPARATUS	4
III	PROCEDURE AND PRELIMINARY EXPERIMENTS	10
IV	WAKE GEOMETRY	
	Fuel-Air Ratio Effect	14
	Mixture Velocity Effect	15
	Variation with Distance from Flameholder	16
	Effect of Flameholder Size	18
V	FLOW FIELDS	
	Static Pressure	20
	Total Pressure	21
	Velocity and Mach Number	23
	Mass Flow	25
VI	CONCLUSIONS	26
	REFERENCES	28
	TABLE	30
	FIGURES	31

LIST OF FIGURES

FIGURE NO.	
1	Time Exposure of a Flame Stabilized on a Circular Cylinder.
2	Schematic Diagram of Flow Systems.
3	16.2 inch Combustion Chamber with 1 inch Diameter Flameholder.
4	Types of Flameholders Used.
5	Schlieren Photograph of Stabilized Flame Indicating "X" and "W" Dimensions.
6	Sketch of Flame Front Boundary Illustrating Method of Determining Wake Widths.
7	Time Exposure of Flame Stabilized by 1 inch Diameter Flameholder.
8	Schlieren Photograph Showing Effect of Longitudinal Pressure Oscillation on Flame Front.
9	Schlieren Photograph Showing Kármán Vortex Type Wake.
10	Composite Schlieren Photograph of Flame Spreading from 1 inch Diameter Flameholder.
11	Composite Schlieren Photograph of Flame Spreading from 1/2 inch Diameter Flameholder.
12	Composite Schlieren Photograph of Flame Spreading from 1/8 inch Diameter Flameholder.
13	Composite Schlieren Photograph of Flame Spreading from 1/16 inch Diameter Flameholder.
14	Wake Width Variation with Fuel-Air Ratio.
15	Wake Width Versus Mixture Velocity, 1/8 inch Diameter Flameholder.
16	Wake Width Versus Mixture Velocity, 1/2 inch Diameter Flameholder.
17	Wake Width Versus Mixture Velocity, 1 inch Diameter Flameholder.
18	Wake Width Versus Distance Downstream of Flameholder, 1/8 inch Diameter.

LIST OF FIGURES (Cont'd)

FIGURE NO.	
19	Effect of Mixture Velocity on Wake Width and Flame Front Slope for Velocities Below the Critical.
20	Wake Width Dependence on Distance for Three Different Diameter Flameholders.
21	Wake Width Dependence on Flameholder Diameter.
22	Pressure Coefficient Versus Mixture Velocity, 1/8 inch Diameter Flameholder.
23	Pressure Coefficient Versus Mixture Velocity, 1/2 inch Diameter Flameholder.
24	Pressure Coefficient Versus Mixture Velocity, 1 inch Diameter Flameholder.
25	Pressure Drop Downstream of Recirculation Zone Versus Distance Downstream of Flameholder.
26	Total Pressure Deficit Across Duct Through Flame Stabilized by 1/8 inch Diameter Flameholder.
27	Normalized Unburnt Gas Velocity Versus Distance Downstream.
28	Mach Number Profile Across Duct at 14 inches Downstream.
29	Fraction of Total Mass Flow in Wake Versus Distance Downstream.

LIST OF SYMBOLS

C_p	pressure coefficient, $(P_s - P_x)/q_s$
D	circular cylinder flameholder
P_s	static pressure in uniform flow upstream of flameholder
P_t	total pressure in plenum chamber
P_{t_y}	total pressure at distance y from the duct centerline and distance x downstream of flameholder
P_x	wall static pressure at distance x downstream of flameholder
q_s	dynamic head in uniform flow upstream of flameholder
q_x	dynamic head in uniform flow at distance x downstream of flameholder
V	approach stream velocity, mixture velocity
W	wake width
X	distance from flameholder reference plane measured downstream
y	distance from duct centerline
$\frac{dW}{dX}$	flame front slope
ρ_b	density of burnt gas
ρ_u	density of unburnt gas
ϕ	fuel-air equivalence ratio, fraction of stoichiometric

I. INTRODUCTION

Present day high output combustion devices such as ramjet engines and turbojet afterburners must handle fuel-air mixtures traveling at velocities of 50-800 feet per second. Since the approach gas velocity is many orders of magnitude greater than the flame speed of the burning gas, the flame must be stabilized or held in the combustion chamber by some physical mechanism. Stabilization can be accomplished by using bluff bodies as flameholders.

Directly behind a bluff body flameholder is a region in which the hot burnt gases recirculate, Fig. 1. This recirculation zone serves as a source of ignition for the total gas stream. The recirculation zone is characterized by small average gas speeds, compared to the approach stream velocity, and high temperatures very near the adiabatic flame temperature. In the immediate wake of the bluff body flameholder is a second region, the mixing zone. In the mixing zone cold combustible material mixes with hot recirculation zone gas. The chemical reaction takes place largely in the mixing zone at the edges of the wake and the recirculation zone gas consists almost entirely of products of combustion. From about the end of the recirculation zone the flame propagates downstream and continues to spread into the unburnt gas.

Much information (1, 2, 3, 4, 5) is available concerning the stability limits of bluff body flameholders, or the range of operating conditions over which a flame can be held on the flameholder. But a knowledge of combustion stability alone is not

enough to characterize a combustion device; a knowledge of combustion efficiency, which depends upon the rate at which the stabilized flame spreads through the remaining unburnt gas, is also of paramount importance. Unfortunately there is little quantitative information available concerning combustion efficiency. Of the few investigations that have been made of flame spreading, most were carried out at low Reynolds numbers in small scale equipment (6, 7, 8). The only extensive investigation made at high Reynolds numbers was that of Petrein, et al. (9) who studied the effect of several geometric and operating variables on combustion efficiency.

The work of Petrein, et al. was valuable in that it gave overall data concerning some of the effects and time average data for efficiency determinations. However, it was felt that an investigation that did not require a time average sampling process to gather data might enable more specific information to be obtained about the mechanism of flame spreading.

This investigation was undertaken with the purpose of determining the dependence of wake width on such variables as fuel-air ratio, flameholder geometry, and approach stream velocity for the region downstream of the recirculation zone, as a first step in gaining better understanding of the mechanism of flame spreading.

The majority of the data was obtained by taking spark Schlieren photographs of the spreading flame through vycor glass

side walls in the combustion chamber. A Schlieren wake width was defined and used throughout the investigation as the principal dependent variable. Investigations of wake width were confined to the range of operating conditions under which a stable flame could be maintained.

II. EXPERIMENTAL APPARATUS

General. The principal features of the flow systems used in these investigations are shown schematically in Fig. 2. A controlled and metered quantity of air was heated to a fixed temperature by a heat exchanger system. Liquid fuel was injected into the hot air stream far enough upstream of the plenum chamber to insure that the combustible mixture entering the combustion chamber was homogeneous. A smoothly convergent nozzle connected the plenum chamber to the combustion chamber; the design of the plenum chamber and the contracting section was adequate to give a uniform flow into the combustion chamber inlet. The combustion chamber was a rectangular duct with a 3" x 6" cross-section. Vycor glass windows, interchangeable with water cooled walls, allowed visual and photographic observation of the flame front throughout the whole length of the combustion chamber. The flame holders were mounted on the center line of the 6 inch wall and were held normal to the incoming flow.

Air Supply and Control System. The air supply for combustion was furnished by two reciprocating pumps with a combined capacity of 3.7 lbs/sec at a pressure of 75 psi. The mass flow rate of air was regulated through a remote controlled sonic-throat valve located upstream of the heat exchanger and fuel injector, allowing control of air flow independent of variations in fuel flow rate, mixture temperature, and changes in combustion chamber static pressure.

Air Temperature Control. The mixture temperature was controlled by shunting a fraction of the air through a conventional shell-and-tube type heat exchanger. The heat exchanger used a turbojet can burner with separate air supply and exhaust as the tube heating element. Two butterfly valves, manually operated, fixed the amount of air passing through the heat exchanger. See Fig. 2. This arrangement made possible quick responses to changes in the gas mixture temperature caused by changes in the fuel-air ratio. A minimum mixture temperature of approximately 195°F was used in all experiments. Complete vaporization of the fuel was thus assured.

Fuel System. The fuel used in these experiments was Standard Oil Thinner No. 200, a gasoline like hydrocarbon fuel whose specifications are given in Table A. This type of fuel was used because it was readily available, easily vaporized, closely controlled in its production, and easily metered as a liquid. The fuel was drawn from tanks which were pressurized to 100 psi by use of nitrogen pressure bottles and injected through a spray nozzle into the air supply line 30 feet upstream of the plenum chamber. This was done to provide adequate time for vaporization and mixing of the fuel and air before the plenum chamber was reached.

Plenum Chamber and Nozzle. The plenum chamber was made up of two parts. The first was a 24 inch diameter pipe section 40.8 inches long. This converged to a 15 by 15 inch square duct over a length of 1.5 inches. The square duct section was 38.7 inches long. To diffuse the high speed air stream entering the plenum chamber,

a 13 inch diameter perforated baffle plate was positioned 3/4 inches downstream of the entrance and two additional 24 inch diameter perforated plates were positioned 24 and 39 inches downstream of the plenum chamber entrance. In the 15 x 15 inch square section of the plenum chamber were two square perforated plates of 75 and 50 per cent blockage, plus two 30 and two 60 mesh screens. These plates and screens served to reduce the turbulence level of the gas stream.

An 8 inch diameter rupture diaphragm was built into the upstream end of the plenum chamber to allow a rapid reduction of pressure in the event of a blow back.

The nozzle was 19 inches long and reduced the flow cross-section from a 15 x 15 inch square duct to a 3 x 6 inch rectangular duct. This gave a contraction ratio of 12.5:1. Pressure surveys of the nozzle showed a flat velocity profile entering the combustion chamber for all operating conditions.

Combustion Chamber. The combustion chamber was a rectangular duct with a 3 x 6 inch cross-sectional flow passage, Fig. 3. Its length could be varied from about 16.2 inches (short duct) to about 45 inches (long duct) by the addition of suitable glass or water cooled metal walls. Vycor glass walls could be interchanged with the water-cooled metal walls to allow visual or photographic observations to be made of the flame front at any station from the flame holder downstream to the end of the duct. Static pressure holes were drilled in the bottom wall of the duct at intervals of one inch

starting from the flame holder mounting plate. This enabled pressure readings to be taken at any desired station. A vertically mounted metal strip one inch wide was used as a mounting plate for the flame holders. This mounting plate was positioned just between the combustion chamber and the nozzle and the apparatus was so constructed that the flame holders could be interchanged without disassembling the duct. The flame holders were mounted through 1/4 inch holes drilled at the vertical centerline of the mounting plates. The discontinuities in the wall surface at the connections between the combustion chamber, the mounting plate, the glass walls or the metal walls were kept less than 0.002 inches.

Flame Holders. The bluff body flame holders primarily used in this investigation were hollow circular cylinders of diameter D. These cylinders were constructed of machined brass rods except for the 1/8 inch diameter cylinder which was constructed of stainless steel tubing. All cylinders were sealed at the ends except for 1/4 inch inlet and outlet tubes used for mounting support and cooling passages.

The holders were mounted in steel plates and were positioned about one inch downstream of the nozzle exit for most runs. On some runs the mounting plates were moved farther downstream in the duct in order to obtain pictures of the flame at intermediate positions. Some typical flame holders used in this investigation are shown in Fig. 4.

Ignition System. A 10,000 volt A. C. spark between the flame holder and an igniter rod was used to ignite the fuel-air mixture. The igniter rod was remotely positioned, and was withdrawn from the combustion chamber after the flame had been established. Ignition was made near the stoichiometric fuel-air ratio at gas speeds up to 200 ft/sec; the larger flame holders were easier to ignite.

Pressure and Temperature Measurements. Plenum chamber pressure and combustion chamber static pressure were measured by both water and mercury manometers. The plenum chamber pressure was obtained from a standard total head tube located on the centerline of the plenum chamber downstream of the last screen. The combustion chamber static pressure was obtained from static pressure orifices located 2 inches downstream of the converging section of the nozzle and about 5 inches upstream of the flame holders. Wall static pressures downstream of the flame holder were measured by water manometers. Temperatures were measured by use of a chromel-alumel thermocouple and a Brown Automatic Potentiometer.

Schlieren Equipment. The Schlieren system used was a conventional double mirror type. A BH-6 lamp light source was used, and the focal lengths of the two 10 inch diameter concave mirrors were 80 inches and 96 inches. Inasmuch as the electrical circuit and the physical layout of the optical system were conventional, no diagrams will be given here. Light flash and the camera

shutter were synchronized by use of several relays arranged in series to furnish the proper time delay between the firing of the shutter mechanism and the Schlieren flash; this arrangement was used to keep the film from being fogged by the light from the flame. Super XX film was used for most pictures and the duration of the spark was less than 7 micro-seconds. A shutter speed of 1/50 of a second was used for all Schlieren pictures.

III. PROCEDURE AND PRELIMINARY EXPERIMENTS

Procedure. In this investigation, spark Schlieren photographs were used to determine the width of the burnt gas wake. On a typical Schlieren photograph, Fig. 5, the flame front is bumpy due to the presence of low amplitude waves or cellular disturbances. These bumps occur in a random pattern and move downstream with the velocity of the unburnt gas mixture. The disturbed zone adjacent to the Schlieren edge of the wake in Fig. 5 consists of unburnt, partially burnt and completely burnt gas. The central portion of the wake which appears on the Schlieren photograph as a transparent region, reasonably free from stria, is presumably a region of burnt gas.

The boundary used in this investigation to determine the wake width was chosen as the locus of the intersections of the bumps on the flame front surface, Fig. 6. By using this boundary instead of the outer edge of the bumps, reproduceable wake widths were obtained which did not vary as the bump heights changed. The dimensions referred to by the wake width, W, and the distance from the flameholder, X, are shown in Fig. 5.

The edge of the wake seen on an ordinary time exposure photograph of the flame, Fig. 7, was found to be identical to the boundary defined by the outer edges of the waves seen on a Schlieren photograph. This outer boundary is referred to as the visual edge of the wake and represents the edge of the zone of the initial temperature rise, Fig. 6.

In order to measure the wake width several photographs were taken at each operating condition and an average wake width for that condition was determined. Variations in the reported data due to the somewhat indefinite nature of the boundary and to errors in measurement after the boundary was chosen were less than $\pm$ 0.05 inches.

Preliminary Experiments. During preliminary investigation of flame spreading in long combustion chambers, several phenomena were observed which caused gross distortions of the flame front. These phenomena were encountered over limited ranges of the variables under investigation and were found to depend strongly on parameters such as combustion chamber length and blockage ratio. Since it was felt that the phenomena were not fundamental features of the flame spreading process, it was decided to study flow regimes for which the distortions were absent.

A longitudinal pressure oscillation in the combustion chamber was the phenomenon that most severely restricted the usable range. Spark Schlieren photographs, Fig. 8, show that when the oscillation is present, the flame front is periodically pinched off into a string of puffs, and high speed Schlieren motion pictures indicate that each of the puffs enclose a pair of vortices. These vortices are shed from the downstream end of the recirculation zone in a symmetric pattern and move downstream with the local gas speed. The vortices were shed at the same frequency as the pressure oscillations; this frequency was always one of the first few modes of the open-open longitudinal oscillation of the combustion chamber.

The range of parameter, within which longitudinal oscillations were important, depended on the geometry of the flow field.

For example, the oscillations became more prevalent and stronger as duct length and blockage ratio were increased, and they tended to be more severe near the limits of flame stabilization. However, the dependence on fuel-air ratio and velocity was less systematic than that observed by Ames (10). The range of fuel-air ratio and velocity, for which the oscillations were observed, was also a strong function of the flameholder geometry.

The mechanism by which the pressure oscillations affect the flame front is thought to be as follows. Vortex shedding is triggered by the passage of the pressure wave through the stagnant gas in the recirculation zone. In turn, the pressure wave is driven by the additional heat release caused by rapid mixing in the shed vortices, or by changes in the coupling between the duct exit and atmosphere.

Efforts were made to suppress the oscillations by changing the location of the flameholder in the duct and by altering the coupling between the exit flow and the atmosphere. As far as could be determined, the presence of the oscillations was not a sensitive function of the flameholder position. During investigation of the influence of exit conditions, it was found that any choking at the downstream end of the duct caused a marked increase in the magnitude of the disturbances and the range of variables over which they were found. In addition, quenching the flame and use of additional flameholders at the duct exit was detrimental.

As the blow-off limits were approached a second type of instability appeared. This disturbance was caused by asymmetric

shedding of vortices from the recirculation zone, Fig. 9. Under these conditions, the flow pattern closely resembled the Kármán vortex street observed under isothermal conditions. In fact, the shedding frequencies were accurately predicted by the work of Roshko (11) when account was taken of the reduced Reynolds number in the hot wake and when the effective wake width rather than the bluff body diameter was used as the characteristic dimension for the Strouhal number. These disturbances were restricted to a narrow range of fuel-air ratios near the blow-off limits and hence were much less important in restricting the usable operating regime than were the longitudinal pressure oscillations.

Because of these two disturbances it was found impossible to use duct lengths greater than 16.2 inches when 1/2' and 1 inch diameter cylinders were employed as flameholders. However, the 1/8 inch diameter flameholder operated smoothly in ducts as long as 45 inches over a wide range of speeds and within a fuel-air ratio band from 0.7 to 1.4 of stoichiometric. Hence, the wake of this flameholder was that investigated most thoroughly.

IV. WAKE GEOMETRY

The general appearance of the wakes of circular cylinder flameholders is indicated in the composite Schlieren photographs of Figs. 10-13. In the figures, the flameholder is at the extreme left-hand side and the flow is from left to right. The top and bottom of each picture was cropped so that the total vertical distance shown is about 4 inches. The photographs show that the wakes spread rapidly in the immediate neighborhood of the holder and more slowly further downstream. The first rapid spread shown by these photographs is primarily a fluid dynamic effect produced by the flow of the approach stream around the bluff body. The geometry of the wake in this region, which includes the recirculation zone, is fairly well understood. The present investigation is concerned with the development of the wake downstream of this initial region. In this section, the dependence of wake width on fuel-air ratio, velocity and flameholder geometry is discussed.

Fuel-Air Ratio. The variation of wake width with fuel-air ratio was found to be small for the circular cylinder flameholders. Fig. 14 shows the character of the variation which was observed; these data were obtained using a 1/2 inch diameter circular cylinder flameholder with a mixture velocity of 220 feet per second. As the fuel-air ratio was increased from lean to stoichiometric the wake width decreased, and as the mixture was made richer the width increased again to a higher value. Although the maximum difference between data obtained at a given station was less than 10 per cent, the variation with fuel-air ratio appeared to be a real, if small, effect.

The data also show that the slope of the flame front, that is (dW/dX), varies slightly with a change in fuel-air ratio. The minimum slope occurred at an equivalence ratio of unity and any increase or decrease from stoichiometric resulted in an increase in the slope of the flame front.

These data for a 1/2 inch cylinder were typical of the results obtained with other size cylinders at approach speeds of the order of 150 feet per second or higher. At very low gas speeds the flame front was laminar and the dependence of wake width on fuel-air ratio was greater.

The investigation was restricted to the range of fuel-air ratios indicated in Fig. 14 because beyond the limiting values shown the longitudinal oscillations and the Kármán vortex disturbances became important. The limiting fuel-air ratios were within 10 to 15 per cent of the blowoff values.

Mixture Velocity. Figs. 15, 16, and 17 show the effect of the mixture velocity on the wake width. These data were obtained using 1/8, 1/2 and 1 inch diameter flameholders with a fuel-air ratio near stoichiometric. The wake width for each cylinder tested was found to be greatest at the lowest velocity investigated. As the velocity was increased the wake widths decreased until a certain transition velocity was reached. At this critical velocity, which varied with the flameholder, the wake widths reached a minimum value and stayed constant as the velocity was further increased. Above the transition point, changing the velocity by a factor of two had no measurable effect on the wake width for any flameholder investigated.

A study of the Schlieren photographs indicated that the critical velocity mentioned above occurred at the transition from laminar to turbulent flow in the flame front. This transition is identical to that observed by Zukoski, (12), in the flame front close to the flameholder. Schlieren photographs indicate that the transition occurs all along the wake boundary at a particular velocity. The transition Reynolds number, based on flameholder diameter and upstream flow conditions, ranged from 1.2×10^4 to 5×10^4 as the diameter changed from 1/8 to 1 inch.

Wake Width Variation with Distance. A study of the wake spreading rate was made with the 1/8 inch flameholder in combustion chambers 16.2, 36 and 45 inches long. The results obtained for speeds greater than the critical and for stoichiometric fuel-air ratio are presented in Fig. 18. The data indicate that the rate of wake spreading was constant for the range of distances downstream that could be investigated.

Data were also obtained in the 16.2 inch combustion chamber for the 1/16, 1/8, 1/2, and 1 inch holders over a wide range of velocities. These results again indicate that, for this more limited range of downstream distances, the spreading was linear even when the velocity was less than the critical. The latter fact is illustrated by data presented in Fig. 19 in which wake widths versus downstream velocity is presented for the 1/16, 1/8, 1/2, and 1 inch holders as a function of downstream distance.

These results are not applicable to the wake in the region of the recirculation zone where the shape is fixed by the rapid

divergence of the flow about the cylinder and the recirculation zone. The distance downstream at which the spreading rate became linear was a function of the blockage ratio; for example it varied from 1 to 3 recirculation zone lengths downstream of the flameholder for the 1 and 1/8 inch cylinder, respectively. Also note that, although the linear character of the wake growth is well established by the data of Figs. 18 and 19, the maximum value of the wake width is less than half of the duct height. Hence, the results discussed here may not be representative of the wake farther downstream. For speeds above the critical, the wake spreading rate was found to be about 0.075 inches per inch for the 1/8 inch diameter holder; the much more limited data available for the 1/2 and 1 inch holders indicate a spreading rate of about 0.05 inches per inch. Note that the spreading rate is very slow; in order for the flame to reach the walls, assuming that the linear spreading rate would continue right to the walls, the duct would have to be about 70 inches long for the 1/8 inch flameholder.

At speeds below the critical value, the spreading rates were strong functions of the velocity, Fig. 19. The spreading rate decreased rapidly as velocity was increased. It might have been expected that below the critical value, the spreading rate would decrease directly with speed; however, no simple correlation could be obtained.

The data of Fig. 18 indicate that the wake widths measured in the short duct were slightly less than those measured in the medium or long ducts although the spreading rates appear to be

identical. It is believed that the difference in wake widths between ducts is due to a difference in the number of water cooled metal walls used upstream of the stations investigated rather than to any dependence on duct length. A similar variation was noted during several tests when the water cooled section of the side wall was increased.

Effect of Flameholder Size. The effect of flameholder size on wake structure is illustrated by composite Schlieren photographs, Figs. 10-13, and by a plot of wake width versus distance for 1/8, 1/2, and 1 inch diameter flameholders, Fig. 20. The photographs and plot show the remarkable fact that at distances farther downstream than the end of the recirculation zone of the 1 inch diameter flameholder, the wake widths differ by less than 30 per cent despite the eight to one variation in flameholder size. This last result is shown more clearly in Fig. 21 in which cross plots of wake width versus flameholder diameter are presented for four different stations downstream. The lack of difference in wake widths indicated in this figure is explained in part by the effects of blockage on the flow field in the immediate wake of the flameholder. Studies by Foster (13) have shown that fluid dynamic effects are predominant in fixing the location of the wake edge bounding the recirculation zone and that the spreading rates are much more rapid at low blockage ratios than at high. The data of Fig. 20 clearly show this result; the wake of the 1/8 inch holder is 7 holder diameters wide at the end of the recirculation zone, $X = 1.8$ inches, while the wake of the one inch diameter holder is only 1.9 diameters wide

at the end of the recirculation zone, X = 7.5 inches.

It is evident from Fig. 20 that the spreading rate of the 1/8 inch holder continued at a high value for some distance downstream of the recirculation zone. This may depend on differences in the velocity gradients in the wakes of the various flameholders. Since the velocity at the wake centerline is zero at the downstream end of the recirculation zone, the velocity gradient is approximately V/0.5W. Thus the initial velocity gradient in a narrow wake is higher than that in a wide wake; if spreading rate depends on this gradient, or the corresponding shear, the narrow wake would be expected to have a higher initial spreading rate.

V. FLOW FIELDS

Static Pressure. Wall static pressure readings could be taken during the course of any run by means of the 0.052 inch diameter holes in the bottom wall of the combustion chamber. Traverses across the duct during a run indicated that the variations in static pressure from wall to wall were less than two per cent of the dynamic pressure; hence the wall pressure is an adequate measure of static pressure in the duct. Static pressures expressed in terms of a pressure coefficient are presented in Figs. 22-24 for the 1/8, 1/2 and 1 inch circular cylinders. The pressure coefficient was defined as $C_p = (P_s - P_x)/q_s$, where P_s is the static pressure in the uniform flow at the combustion chamber entrance, P_x is the wall static pressure at a distance X downstream of the flameholder, and q_s is the dynamic head in the uniform flow at the duct entrance. The pressure coefficients presented in Figs. 22-24 are for the burning condition; thus they are roughly ten times larger than for the cold flow condition.

The pressure coefficient was found in general to be larger at low speeds and to decrease rapidly as the velocity increased to the critical value. For speeds greater than the critical value, the pressure coefficient flattened out and the difference in coefficients between any two stations approached a constant value.

The latter effect is shown more clearly by plotting the difference between static pressure coefficients measured at the station located at the downstream end of the recirculation zone and other stations located farther down the duct. The 1/8 inch data, plotted in the above manner, are presented in Fig. 25.

This plot shows that the pressure drop is directly proportional to the upstream dynamic head, q_s, for stations farther downstream than about 4 inches and at velocities higher than the critical value. At velocities above the critical value the region 4 inches downstream and beyond is also the region in which the wake spreading rate is linear and independent of velocity.

Total Pressure. Total pressure measurements were made during runs with the 1/8 inch cylinder. Results obtained at three stations, 2, 8 and 13 inches downstream, and at a velocity of 292 feet per second are shown in Fig. 26 in terms of normalized total pressure deficit versus the distance from the centerline, y. The normalized total pressure deficit was defined as $(P_{t_y} - P_t)/q_s$, where P_{t_y} is the total head at a particular location, (x, y), P_t is the total head in the plenum chamber, and q_s is the dynamic pressure upstream of the flameholder.

The total pressure was constant in the unburnt flow, except for wall boundary layers, but decreased rapidly once the wake boundary was reached. The initial pressure drop occurred at the visual flame boundary, slightly outside the wake width boundary, and the total head dropped off very rapidly through the disturbed region at the edge of the wake. Between the disturbed regions, the total head deficit was constant. This general picture was correct for all stations downstream of the flameholder. However, for stations close to the holder, the disturbed region at either wake edge overlapped at the duct centerline and hence the region of constant total head was not observed.

The minimum normalized total head deficit in the central region was roughly 1.1 and was independent of station or approach stream velocity. The order of magnitude of this loss is easily explained by the following analysis. The flame front, in a high speed flow, is inclined at a very small angle with respect to the streamlines because the flame speed is so much less than the local gas speed.

In passing through the flame front a fluid element undergoes a large density change and a negligible change in static pressure and velocity. Hence, the change in total head is a result of the change in dynamic pressure alone and is given by $P_t = q_x(1-\rho_b/\rho_u)$. Here q_x is the local dynamic pressure of the unburnt gas, and ρ_b and ρ_u are the burnt and unburnt gas densities. Since the density ratio is of the order of 1/5 for the fuel-air ratios used in this experiment, the total pressure loss due to combustion alone is of the order of $(0.85\ q_x)$. Note that the observed loss is about $(1.1\ q_s)$ which is of the expected magnitude. However, the observed loss was found to be proportional to the upstream static pressure and not the local value. This is surprising because the local value may be as much as fifty per cent greater than the upstream value. The analysis and experimental results show that the greater part of the observed total head loss is a result of the combustion process and that the flameholder drag is of little importance in fixing the total head wake.

Interpretation of the total head measurements in the disturbed region was difficult because of the non-steady character of the flow. Thus, at a fixed point, the local velocity remained

relatively constant, although the density fluctuated rapidly as masses of burned and unburned material passed the point. The fluctuating density caused a corresponding fluctuation in the dynamic pressure and hence in the total pressure. The total head measurements presented in Fig. 26 therefore represent an average value in the disturbed region; the nature of the average depends on the acoustic properties of the probe and was not investigated. Schlieren photographs showed that except for the disturbed region the flow was steady. Hence the measured values in the steady flow regions are believed to be reliable, although total pressure measurements were also time averages.

Velocity and Mach Number. The velocity and Mach number fields for the flow outside the wake was established by the corresponding total and static pressure fields. Pressure data showed that the Mach number and velocity profiles in the unburnt mixture were essentially flat between the wall boundary layer and the visual wake boundary. The velocity and Mach number increased rapidly with distance downstream from the flameholder due to the pressure drop down the duct. The nature of this increase is illustrated in Fig. 27 for the 1/8 inch holder wake. In this example, the velocity of the unburnt gas outside the wake was about 35 per cent faster 15 inches downstream than at the duct entrance.

Accurate determination of Mach number and velocity inside the wake was impossible because the temperature profile was unknown. However, the Mach number, which is a function of the temperature because of its dependence on the specific heat ratio, could

be reasonably estimated given values of the total and static pressure. Fig. 28 illustrates the variation of Mach number across the duct at the 14 inch station for the 1/8 inch holder. The operating condition used was the same as that used to obtain the total pressure data of Fig. 26. As would be expected, the Mach number drops off steeply at the wake edge and is almost constant in the undisturbed flow near the duct centerline.

A determination of the velocity inside the wake is much more difficult due to the fact that the velocity dependence on the assumed temperature profile is very great. However, a qualitative idea of the velocity may be obtained by observing the stria on the wake boundary as shown in Fig. 12. Note that up to about 6 inches from the flameholder the bumps on the flame surface appear to "roll" in the direction of the flow and into the wake. Past 6 inches, however, the bumps appear to "roll" upstream towards the flameholder. As the velocity of the burnt gas inside the wake increases, the inclination of the stria from inside the wake to the wake surface gradually changes from an inclination that is directed downstream, to a vertical position (indicating that the burnt gas and the unburnt gas have the same velocity), and finally to an inclination that is directed back upstream towards the flameholder. Thus it can be seen that while the mixture velocity outside the wake increased 35 per cent in 15 inches the velocity of the burnt gas inside the wake increased even more in the same distance. If the temperature at the wake centerline is assumed to be the adiabatic flame temperature, the Mach number plot of Fig. 28 can be interpreted as indicating that the centerline velocity is about fifty per cent greater than that of the unburnt mixture at the station investigated.

Mass Flow. To determine the mass flow inside the wake as a function of distance, the mass flow outside the wake was determined at several stations and was subtracted from the total mass flow entering the combustion chamber. Because the data were obtained by taking the difference of two large numbers, great accuracy cannot be expected. Fig. 29 shows a plot of the fraction of the total mass in the wake as a function of distance down the duct. As can be seen from the figure the influx rate appears to be constant for the distance investigated.

The static and total head data show that, outside the wake, the velocity at a particular station is almost directly proportional to the velocity upstream of the flameholder. This result coupled with the fact that the wake width is also independent of upstream velocity implies that the mass flow into the wake must be directly proportional to the upstream velocity. Hence, the data of Fig. 29 are typical of mass flows in the wake for all velocities as long as the flame front is turbulent.

CONCLUSIONS

The data presented in this report have established the following picture of the burning wake of a bluff body flameholder. In the region including the flameholder and the recirculation zone the wake boundary is fixed by the pressure field caused by flow around the bluff body. Farther downstream, the wake spreading rate is small and for a given flow condition is independent of distance from the flameholder. For a turbulent wake the location of the wake boundaries is independent of the upstream mixture velocity and only weakly dependent on the fuel-air ratio, and the total pressure deficit and the static pressure coefficient for a turbulent wake are weakly dependent on these parameters. However, for a laminar flame front the wake width and pressure coefficients are strongly dependent on both the mixture velocity and fuel-air ratio.

The spreading rate of a turbulent wake has been found to increase slightly as the fuel-air ratio is changed from stoichiometric. This result is hard to reconcile with the fact that laminar flame speeds decrease rapidly at fuel-air ratios on either side of stoichiometric. However, other experiments with turbulent flames and some theoretical analysis, (14), give an indication that the propagation rate of lean or rich turbulent flames may be greater than that of a stoichiometric flame.

The total pressure profile across the wake is largely fixed by combustion processes which cause losses large enough to completely obscure the deficit associated with flameholder drag. Because the combustion losses are continuously produced, the maximum total pressure deficit remains constant at stations far downstream

of the flameholder. The total head loss produced by the drag is contained within the combustion wake and apparently is unimportant in fixing the spreading of the wake.

The strong influence of blockage is shown by the difference in wake spreading rates near the flameholder for high and low blockage holders. This influence is at least partially responsible for the remarkably weak dependence of wake width on flameholder size. However, the higher spreading rates observed downstream of small holders cannot be explained entirely in terms of blockage effects and must be partially due to the nature of the flow field in the wake itself.

REFERENCES

1. Zukoski, E. E., and Marble, F. E.: "Some Experiments Concerning the Mechanism of Flame Stabilization on Bluff Bodies," Proceedings of the Gas Dynamics Symposium, Northwestern University Press, (August 1955).

2. Wright, F. H.: "Composition Distribution in a Flame Held by a Bluff-Body Flameholder," Report No. 20-286, Jet Propulsion Laboratory," Pasadena, (February 1956).

3. Longwell, J. P., Frost, E. E., and Weiss, M. A.: "Flame Stability in Bluff Body Recirculation Zones," Industrial and Engineering Chemistry, vol. 45, Washington, American Chemical Society, (1953), pp. 1629-1633.

4. Westenberg, A. A., Berl, W. L., and Rice, J. L.: "Studies of Flow and Mixing in the Recirculation Zone of Baffle-Type Flameholders," Johns Hopkins University Applied Physics Laboratory,"CM-844 (June 1955).

5. Zukoski, E. E., "Review of Information Concerning Flame Stabilization on Bluff Bodies," Progress Report No. 20-220, JPL, Pasadena, (April 1954).

6. Berl, W. G., Rice, J. L., and Rosen, P.: "Stabilized Flames in Turbulent Streams," Paper 155-54 presented at ARS Ninth Annual Meeting, New York, (1954).

7. Wilkerson, E. C., and Fenn, J. B.: "The Effect of Flameholder Geometry on Combustion Efficiency in Ducted Burners," Fourth Symposium on Combustion, Williams and Wilkins, Baltimore (1953), p. 749.

8. Williams, G. C., Hottel, H. C., and Scurlock, A. C.: "Flame Stabilization and Propagation in High Velocity Gas Streams," Third Symposium on Combustion, Williams and Wilkins, Baltimore (1949), p. 21.

9. Petrein, R. J., Longwell, J. P., and Weiss, M. A.: "Flame Spreading from Baffles," Jet Propulsion, Vol. 26, Easton, American Rocket Society (February 1956).

10. Ames, L. E., Jr.: "Interference Effects Between Multiple Bluff Body Flameholders," Thesis, California Institute of Technology, Pasadena, (June 1956).

11. Roshko, A.: "On the Development of Turbulent Wakes from Vortex Streets," NACA TN 2913, Washington (March 1953).

12. Zukoski, E. E.: "Flame Stabilization on Bluff Bodies at Low and Intermediate Reynolds Numbers," Thesis, California Institute of Technology, Pasadena, (June 1954).

REFERENCES (Cont'd)

13. Foster, J. R.: "Effects of Combustion Chamber Blockage on Bluff Body Stabilization," Thesis, California Institute of Technology, Pasadena, (June 1956).

14. Mickelsen, W. R., and Ernstein, N. E.: "Growth Rates of Turbulent Free Flames", Sixth Symposium on Combustion, Reinhold Publishing Corporation, New York, (1957), p. 331.

TABLE A

Properties of Hydrocarbon Fuel Used in This Investigation

1.	Heat of combustion, net	18,675 BTU/lb	
2.	Average molecular weight	96	
3.	Latent heat of vaporization at 77°F	148 BTU/lb	
	Vapor pressure at 100°F	2.5 psi	
4.	Density, specific at 60°F	0.7366	
	Density, lb/gal at 60°F	6.132 lb/gal	
5.	Hydrocarbon type analysis	Saturates	94.5%
		Olefins	00.5%
		Aromatics	5.0%

6. Distillation Astm

Initial	172°F
5	179
10	180
20	183
30	186
40	188
50	191
60	195
70	198
80	202
90	208
95	214
Dry	224

7. Chemical Analysis. (Proportions by weight)

Carbon	Hydrogen
85.4%	14.6%

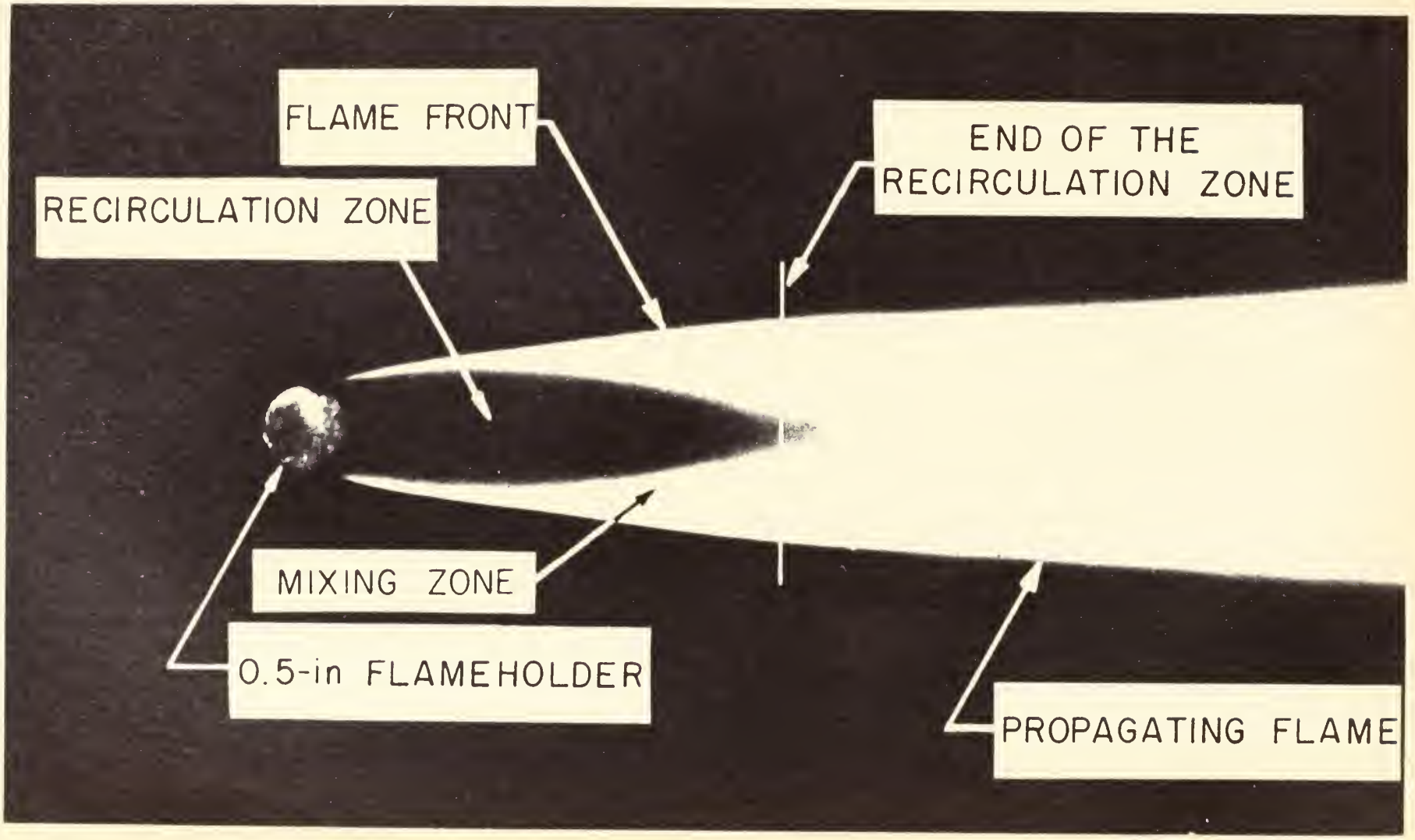

Figure 1. Time Exposure of a Flame Stabilized on a Circular Cylinder

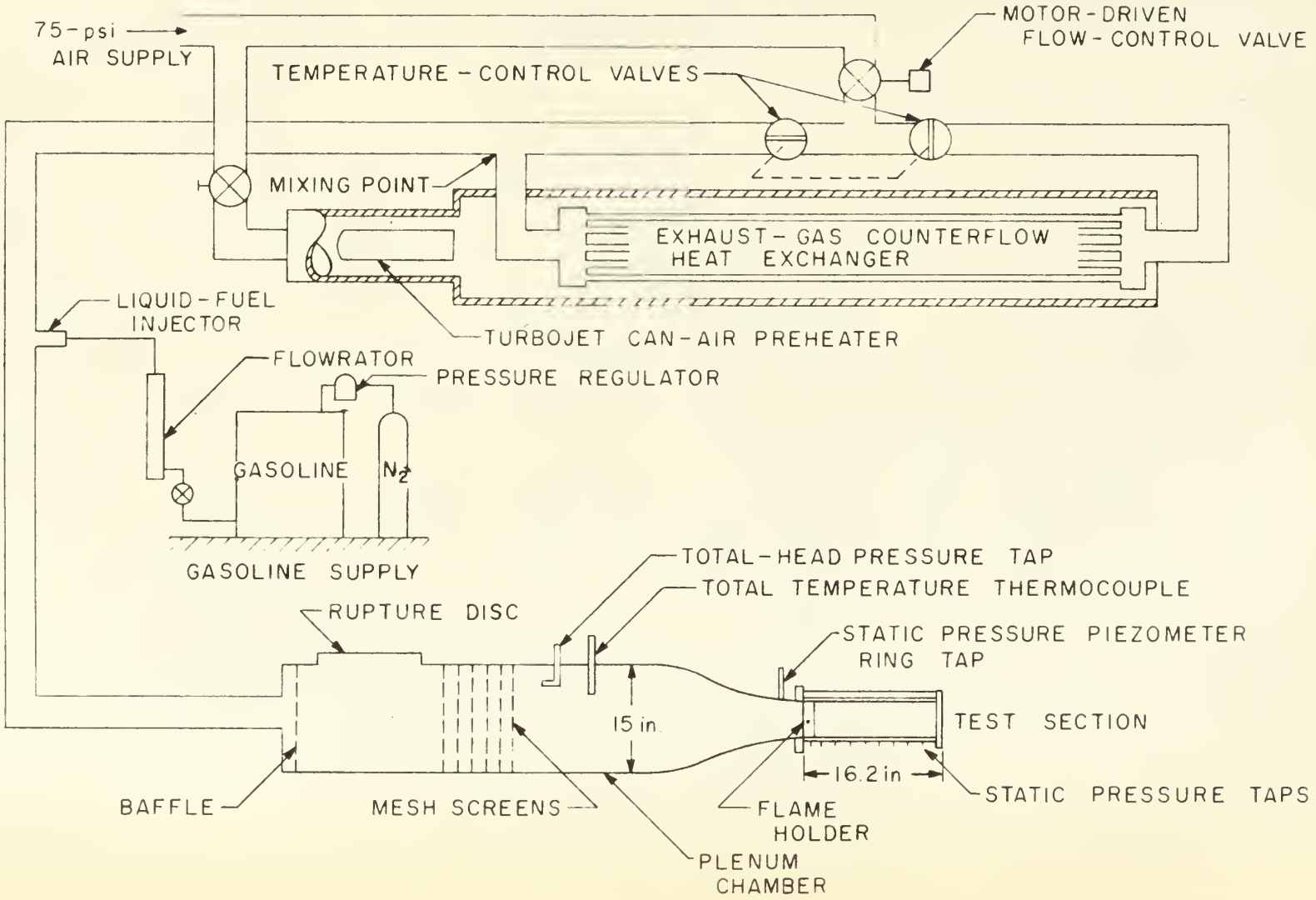

FIGURE 2. SCHEMATIC DIAGRAM OF FLOW SYSTEMS

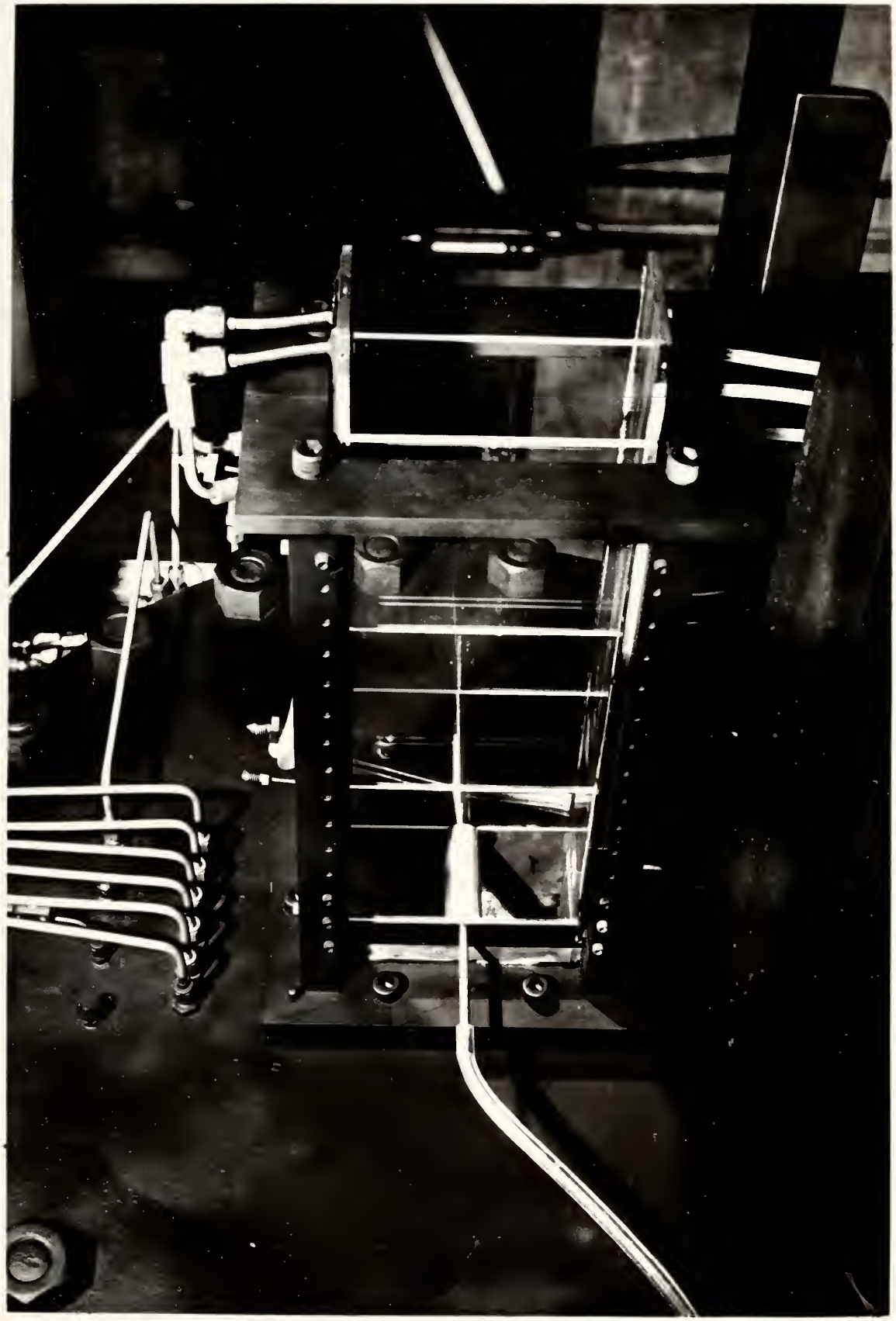

Figure 3. 16.2 inch Combustion Chamber with 1 inch Diameter Flameholder

Figure 4. Types of Flameholders Used

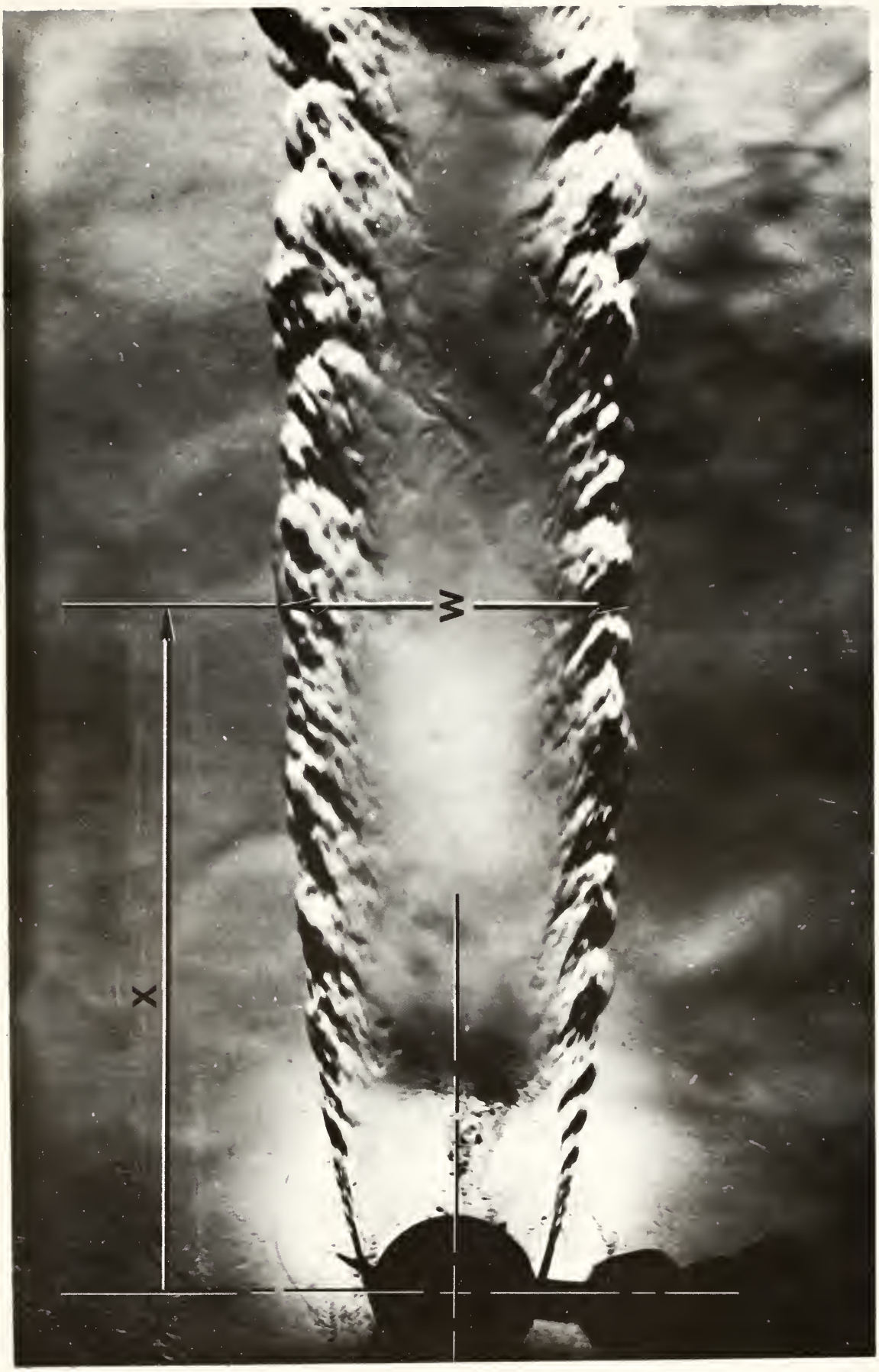

Figure 5. Schlieren Photograph of Stabilized Flame Indicating "X" and "W" Dimensions

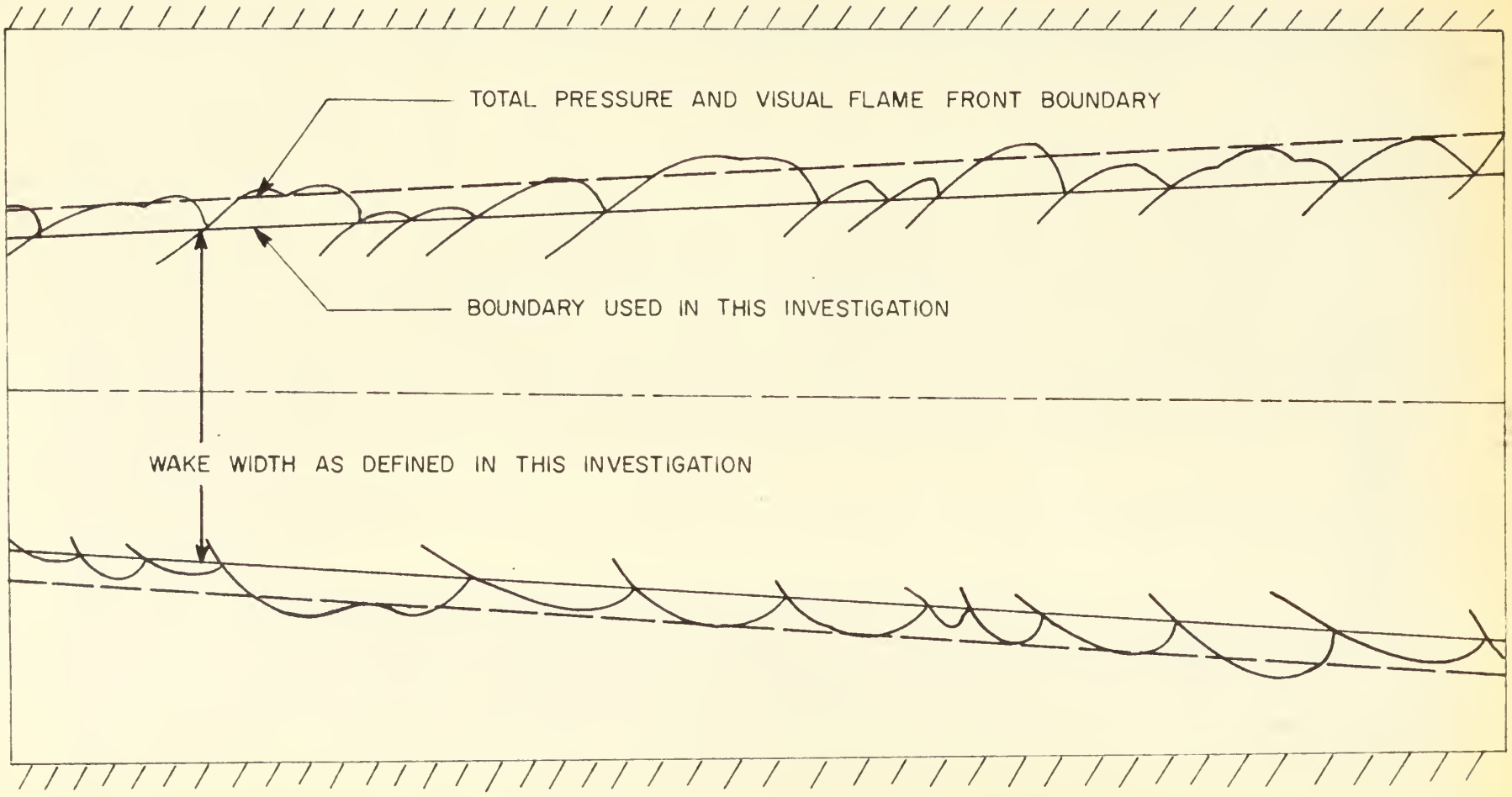

Figure 6. Sketch of Flame Front Boundary Illustrating Method of Determining Wake Widths Used in This Investigation.

Figure 7. Time Exposure of Flame Stabilized by 1 inch Diameter Flameholder

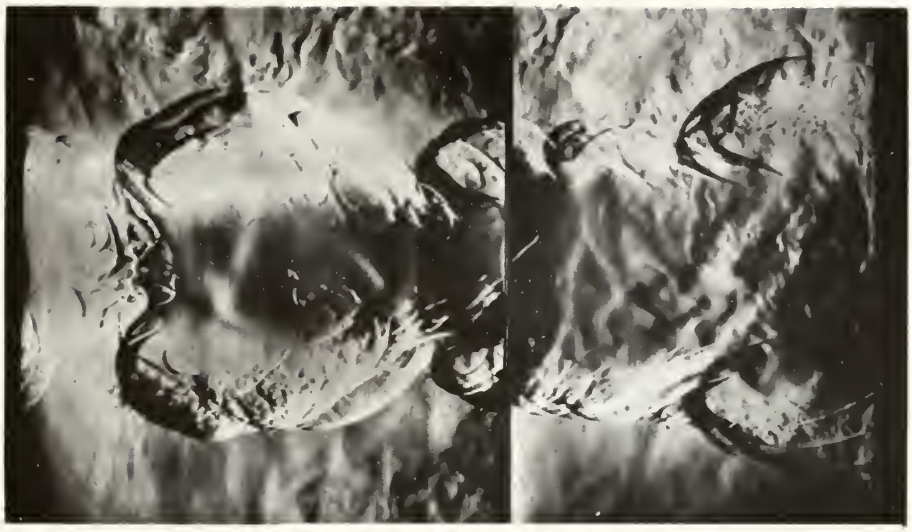

Figure 8. Schlieren Photograph Showing Effect of Longitudinal Pressure Oscillation on Flame Stabalized by 1/8 inch Diameter Flameholder; ϕ = 1.0, 277 ft/sec Mixture Velocity. Photograph includes stations 9-15 inches in the 16.2 inch Combustion Chamber.

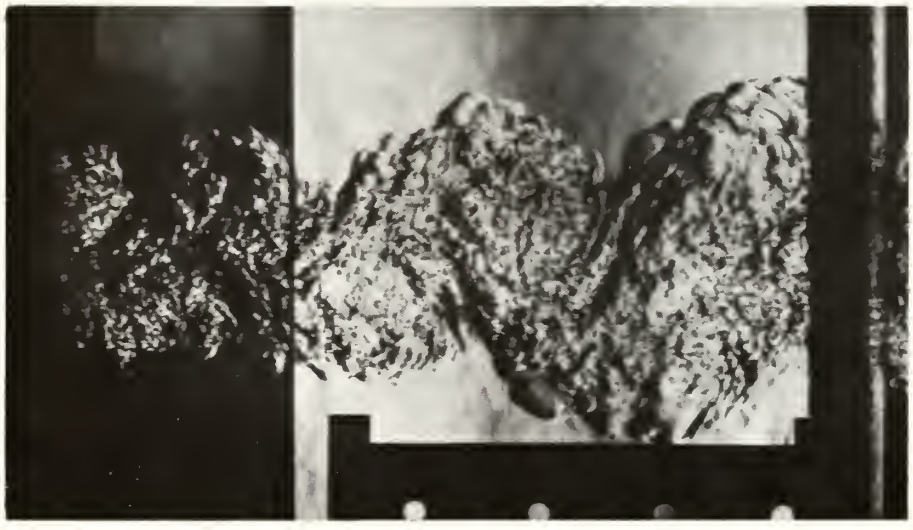

Figure 9. Schlieren Photograph Showing Kármán Vortex Type Wake Obtained Near Lean Blowoff Limit for Flame Stabalized by 1/2 inch Diameter Flameholder; ϕ = 0.65, 214 ft/sec Mixture Velocity. Photograph includes stations 9-15 inches in the 16.2 inch Combustion Chamber.

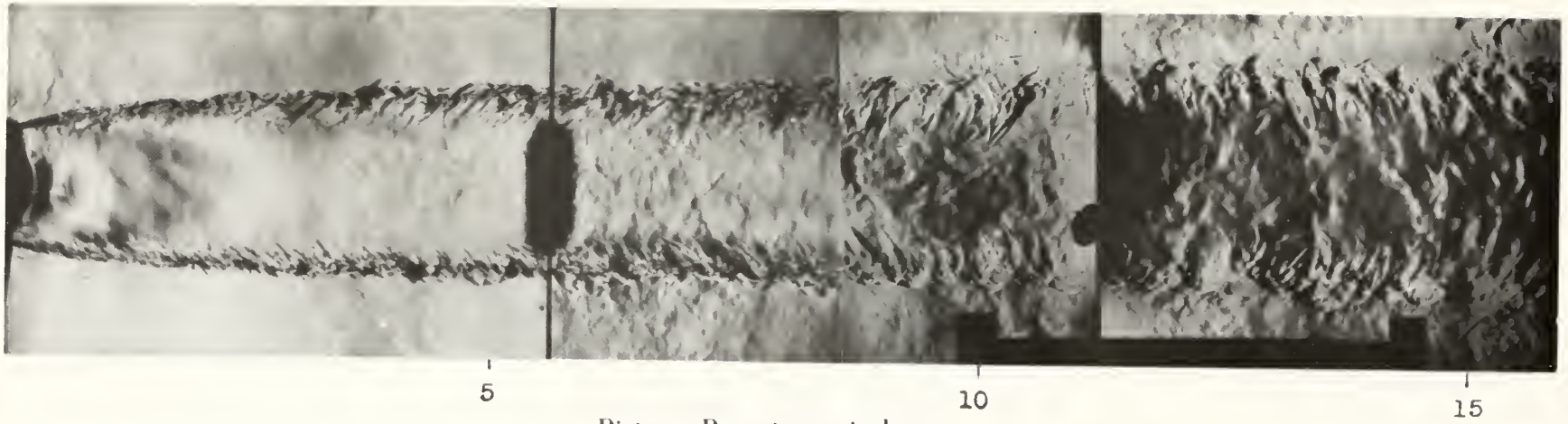

Distance Downstream, inches

Figure 10. Composite Photograph of Flame Spreading from 1 inch Diameter Flameholder; ϕ = 1.0, 300 ft/sec Mixture Velocity

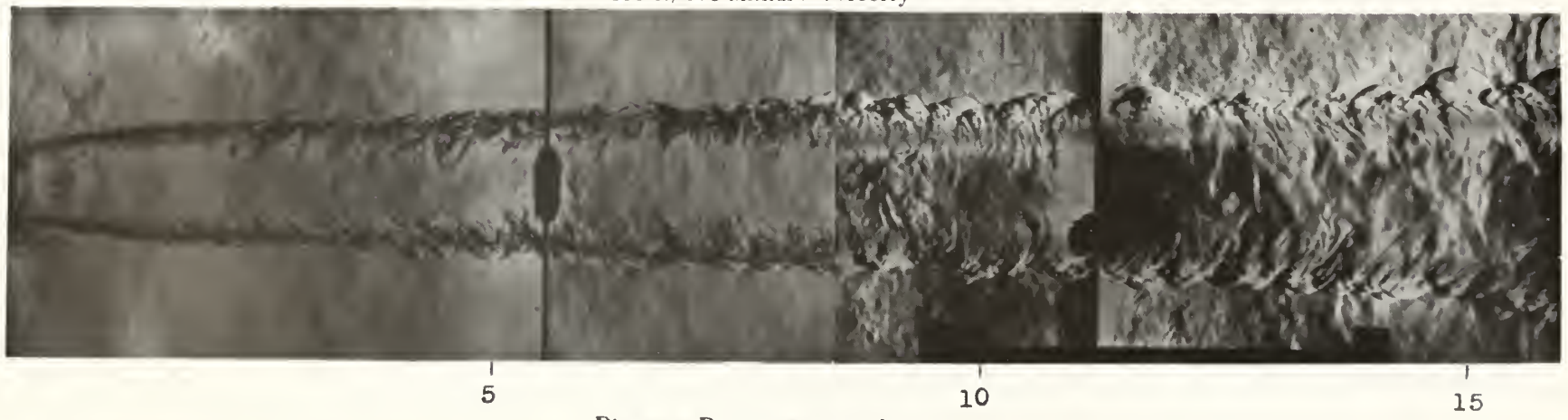

Distance Downstream, inches

Figure 11. Composite Photograph of Flame Spreading from 1/2 inch Diameter Flameholder; ϕ = 1.0, 300 ft/sec Mixture Velocity

18064
G

Figure 12. Composite Photograph of Flame Spreading from 1/8 inch Diameter Flameholder; ϕ = 1.0, 300 ft/sec Mixture Velocity

Figure 13. Composite Photograph of Flame Spreading from 1/16 inch Diameter Flameholder; ϕ = 1.0, 193 ft/sec Mixture Velocity

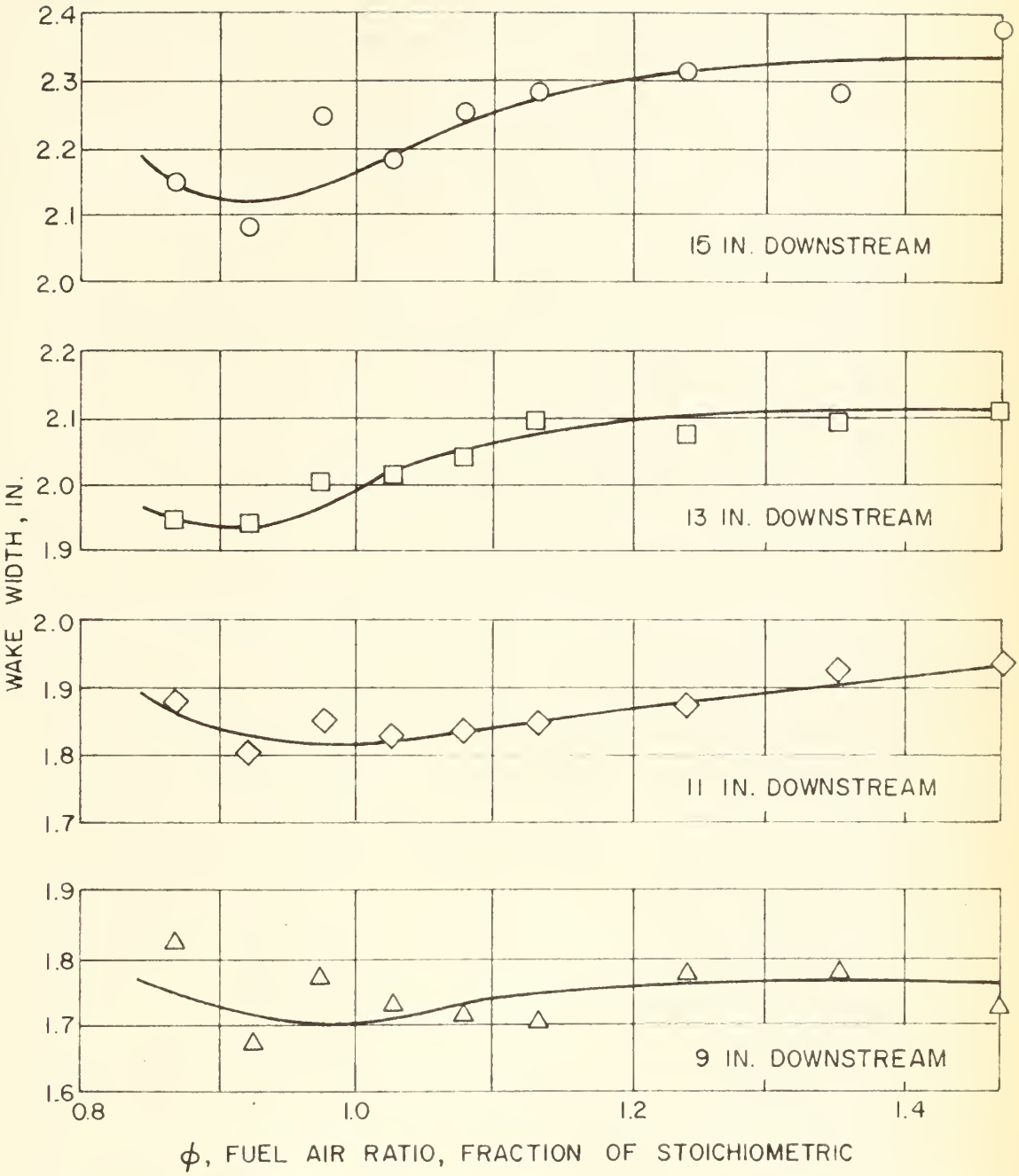

Figure 14. Wake Width Variation with Fuel-Air Ratio, 1/2 Inch Diameter Flameholder, 220 ft/sec Mixture Velocity.

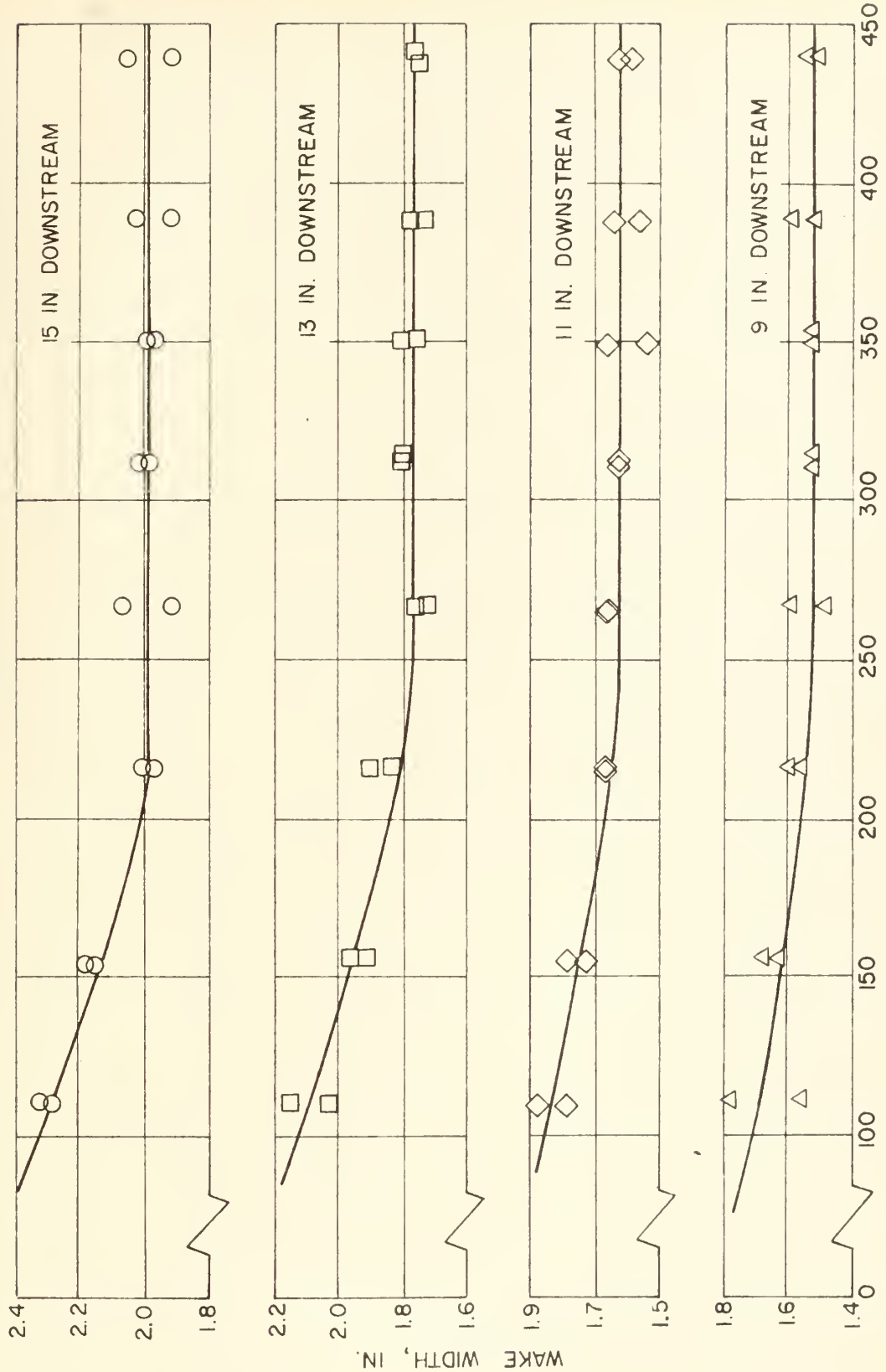

Figure 15. Wake Width Versus Mixture Velocity at Various Downstream Stations; $\phi = 1.0$, 1/8 inch Diameter Flameholder.

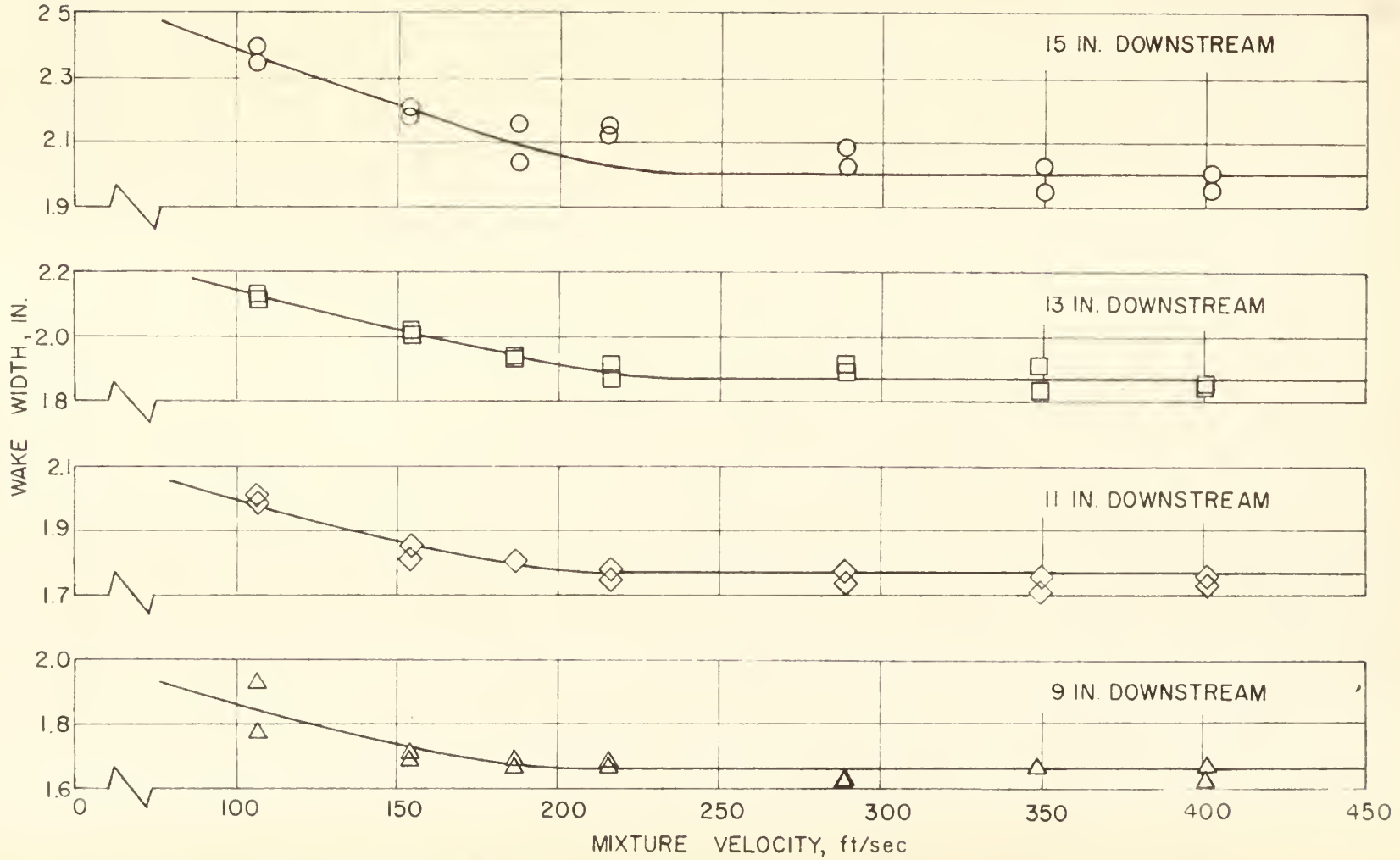

Figure 16. Wake Width Versus Mixture Velocity at Various Downstream Stations; ϕ = 1.0, 1/2 inch Diameter Flameholder.

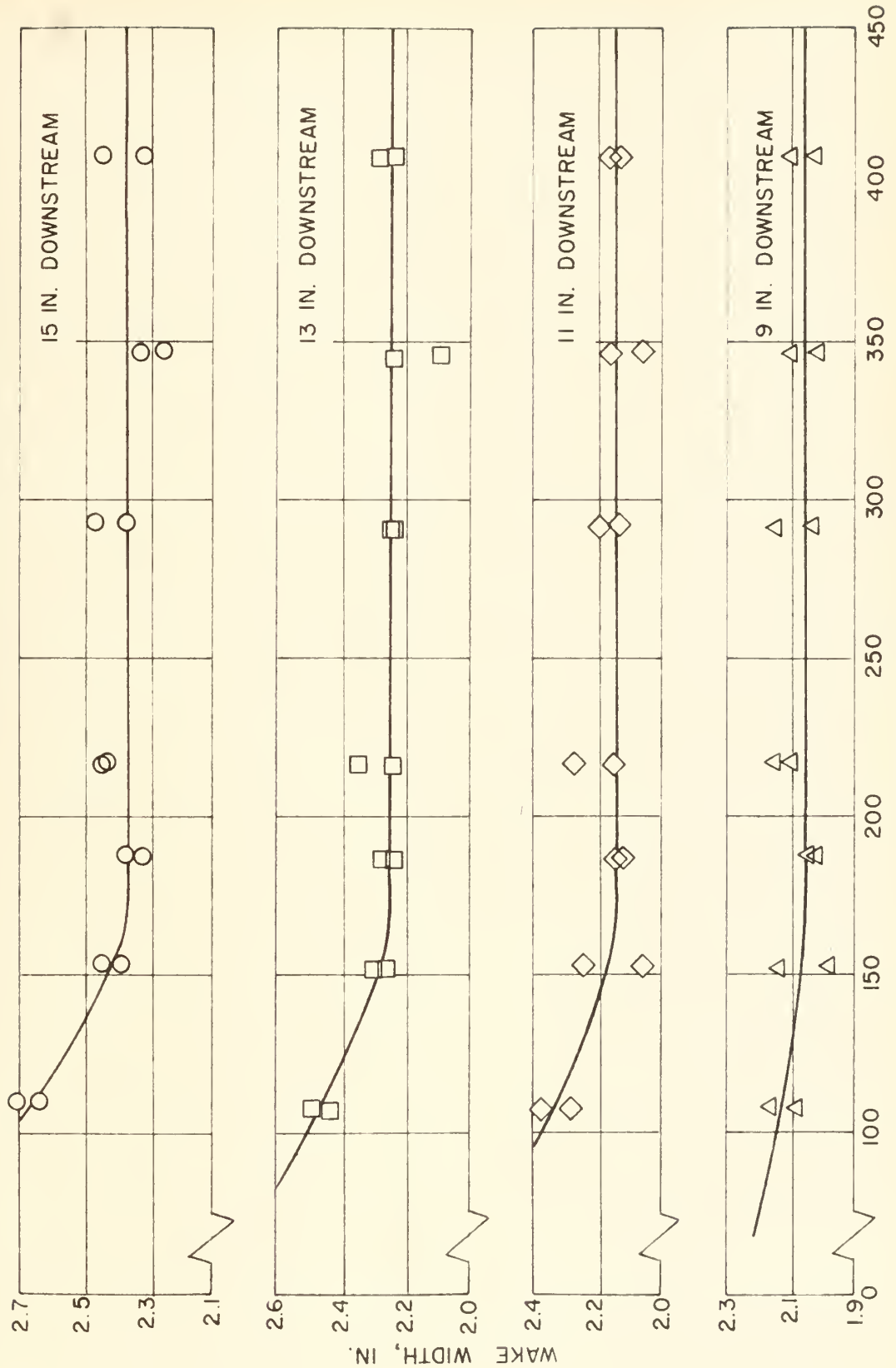

Figure 17. Wake Width Versus Mixture Velocity at Various Downstream Stations; $\phi = 1.0$, 1 inch Diameter Flameholder.

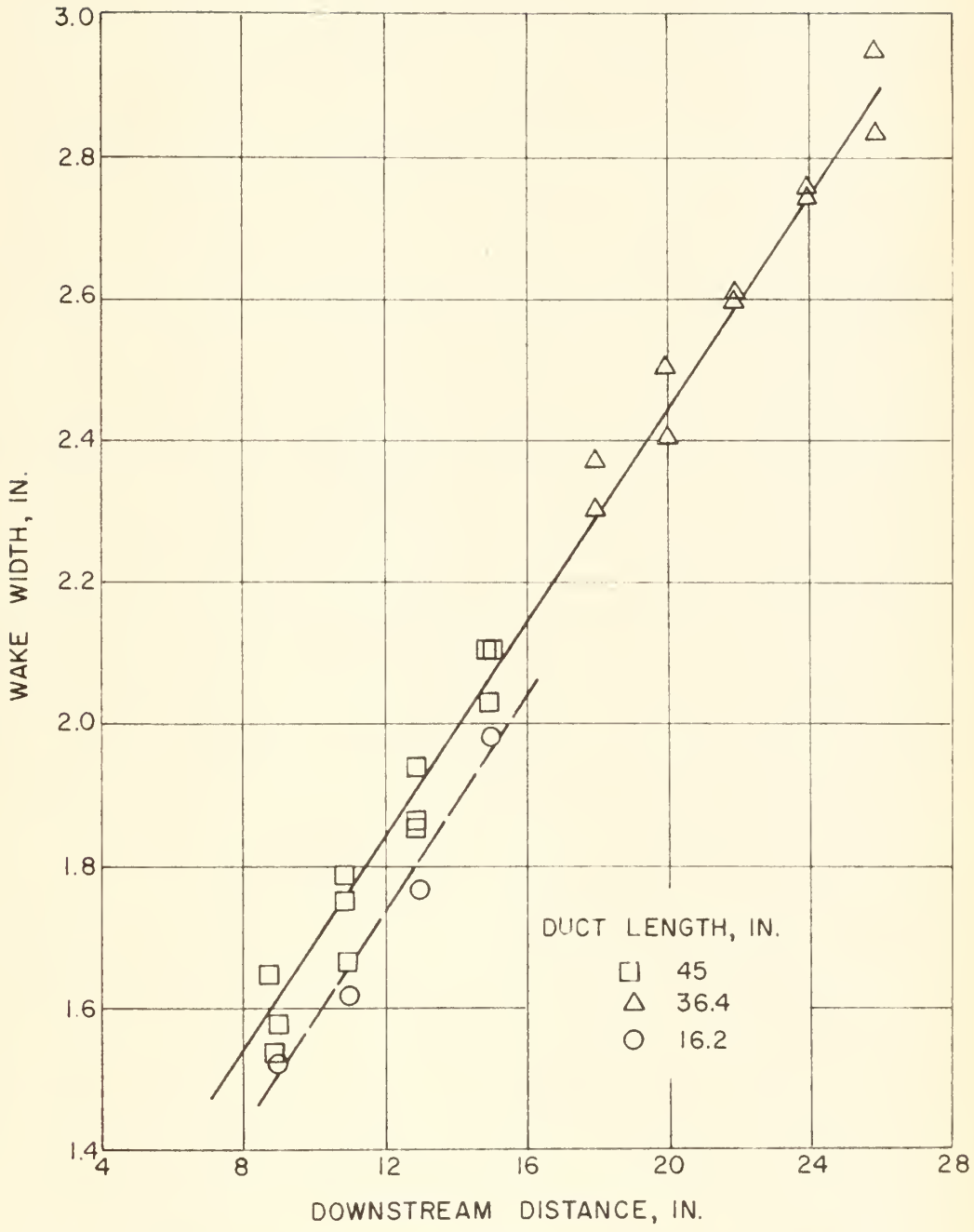

Figure 18. Wake Width Variation with Downstream Distance; $\phi = 1.0$, 300 ft/sec Mixture Velocity.

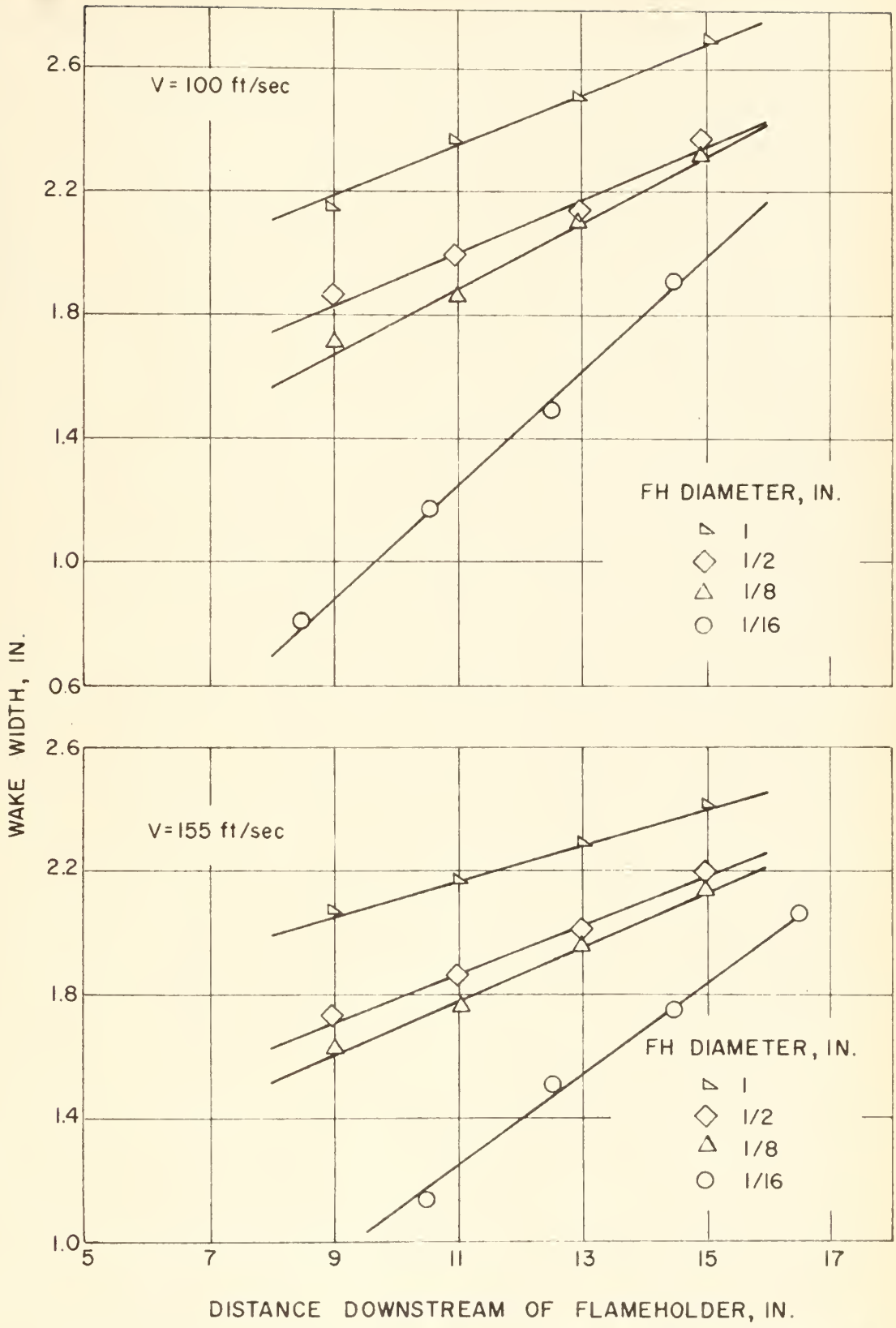

Figure 19. Effect of Mixture Velocity on Wake Width and Flame Front Slope; $\phi = 1.0$.

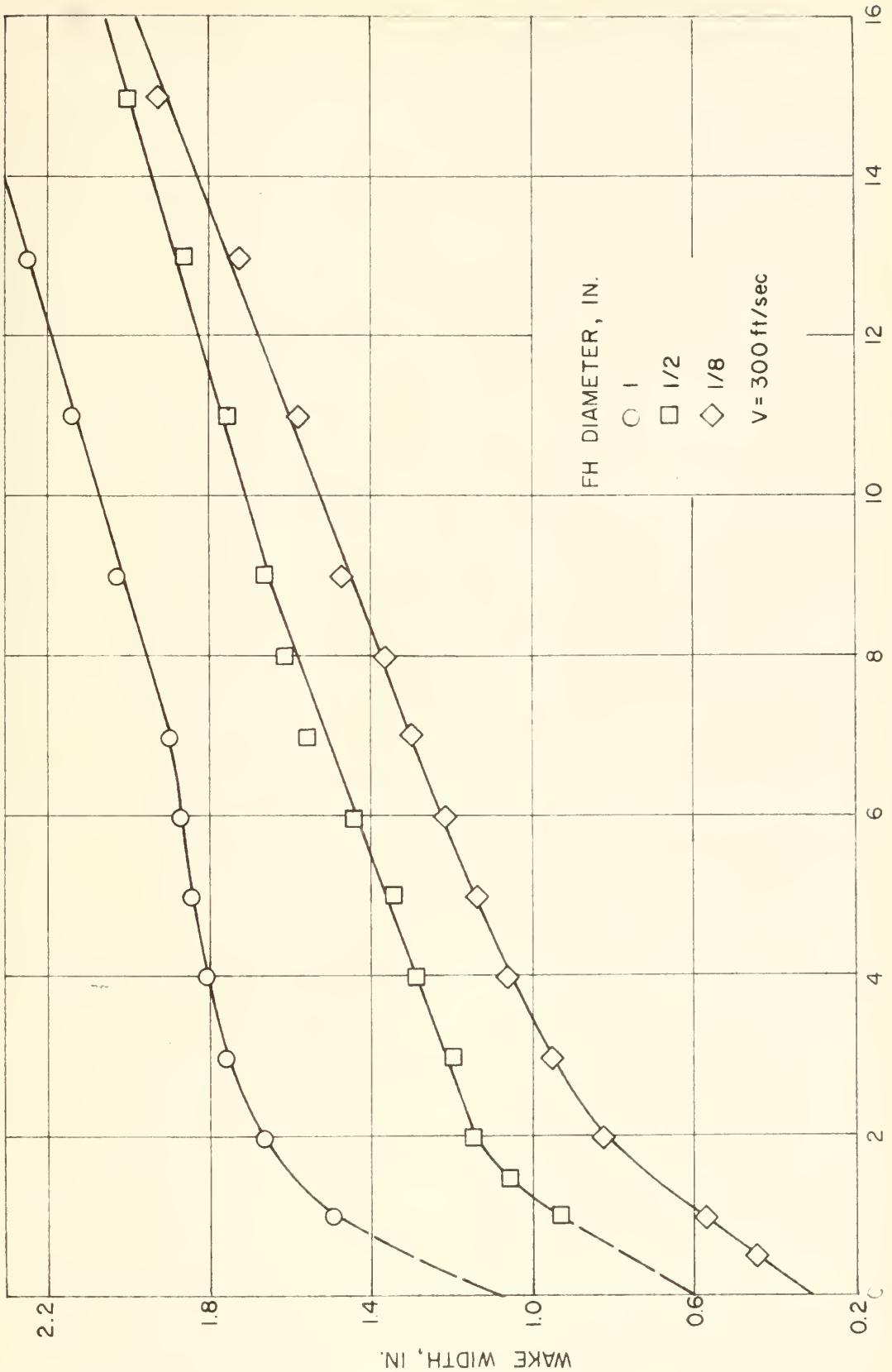

Figure 20. Wake Width Versus Distance Downstream for Three Different Flameholders; $\phi = 1.0$.

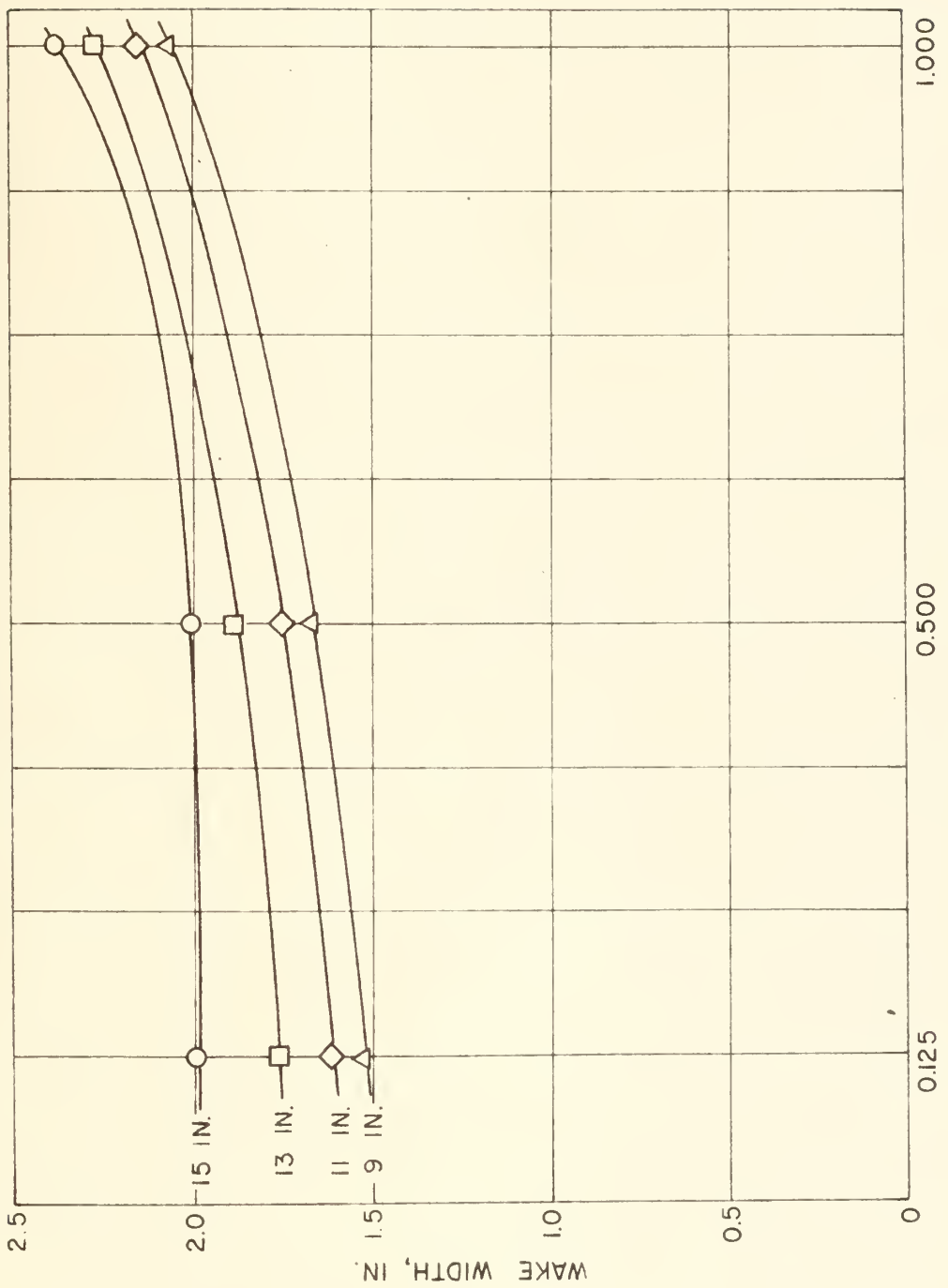

Figure 21. Wake Width Versus Flameholder Diameter, $\phi = 1.0$.

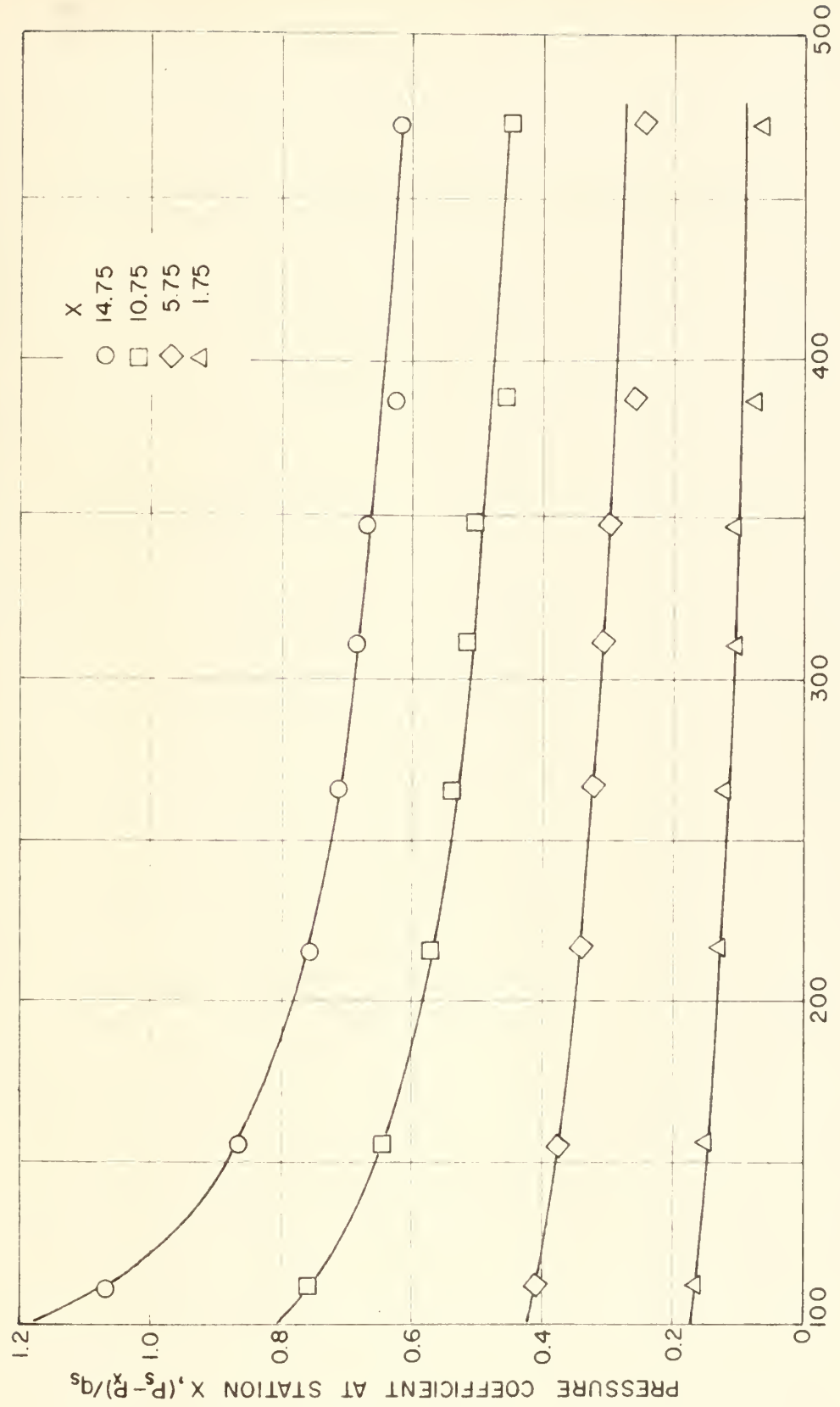

Figure 22. Pressure Coefficient Versus Mixture Velocity at Various Stations Downstream; $\phi = 1.0$, 1/8 inch Diameter Flameholder.

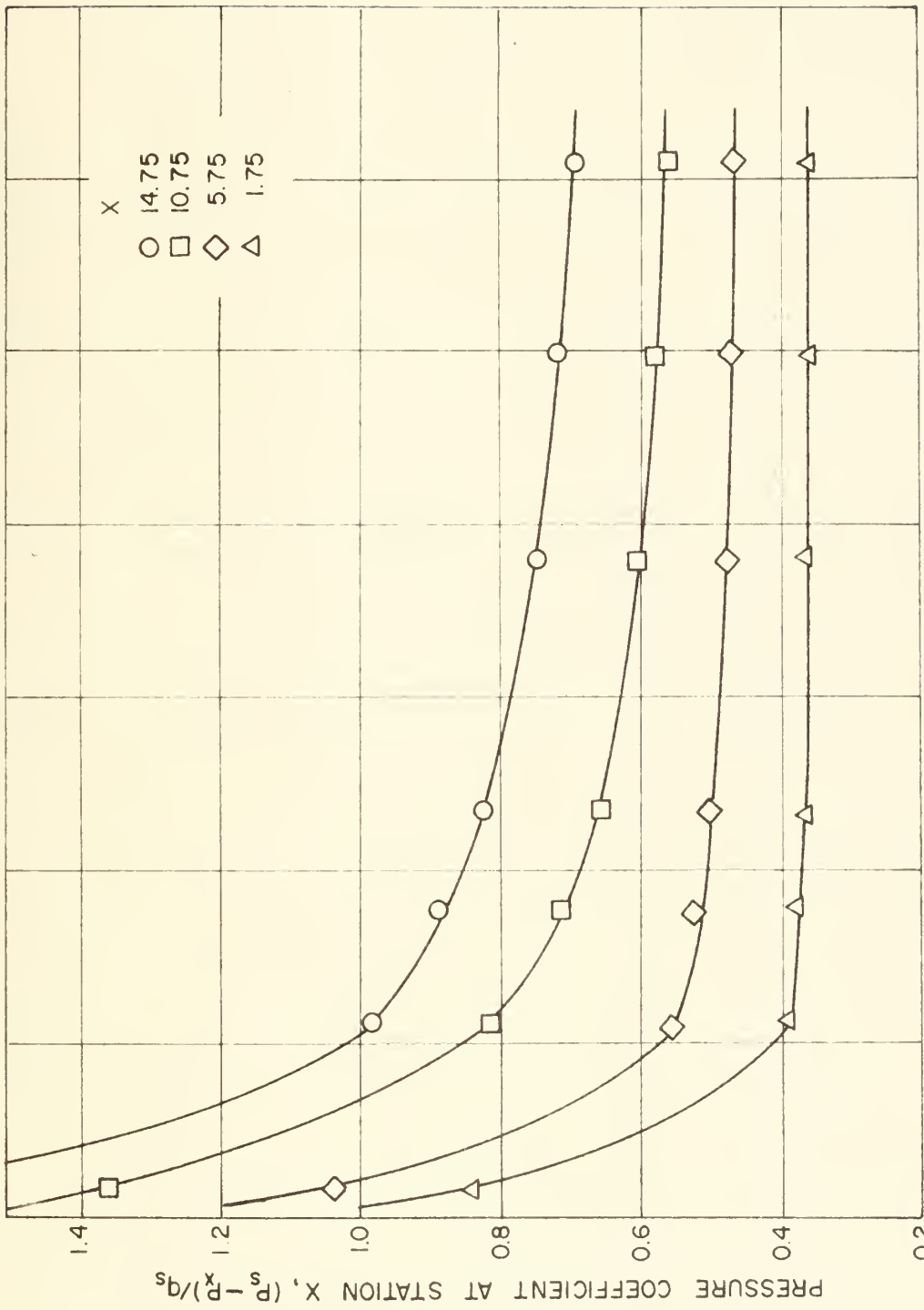

Figure 23. Pressure Coefficient Versus Mixture Velocity at Various Stations Downstream; $\phi = 1.0$, 1/2 inch Diameter Flameholder.

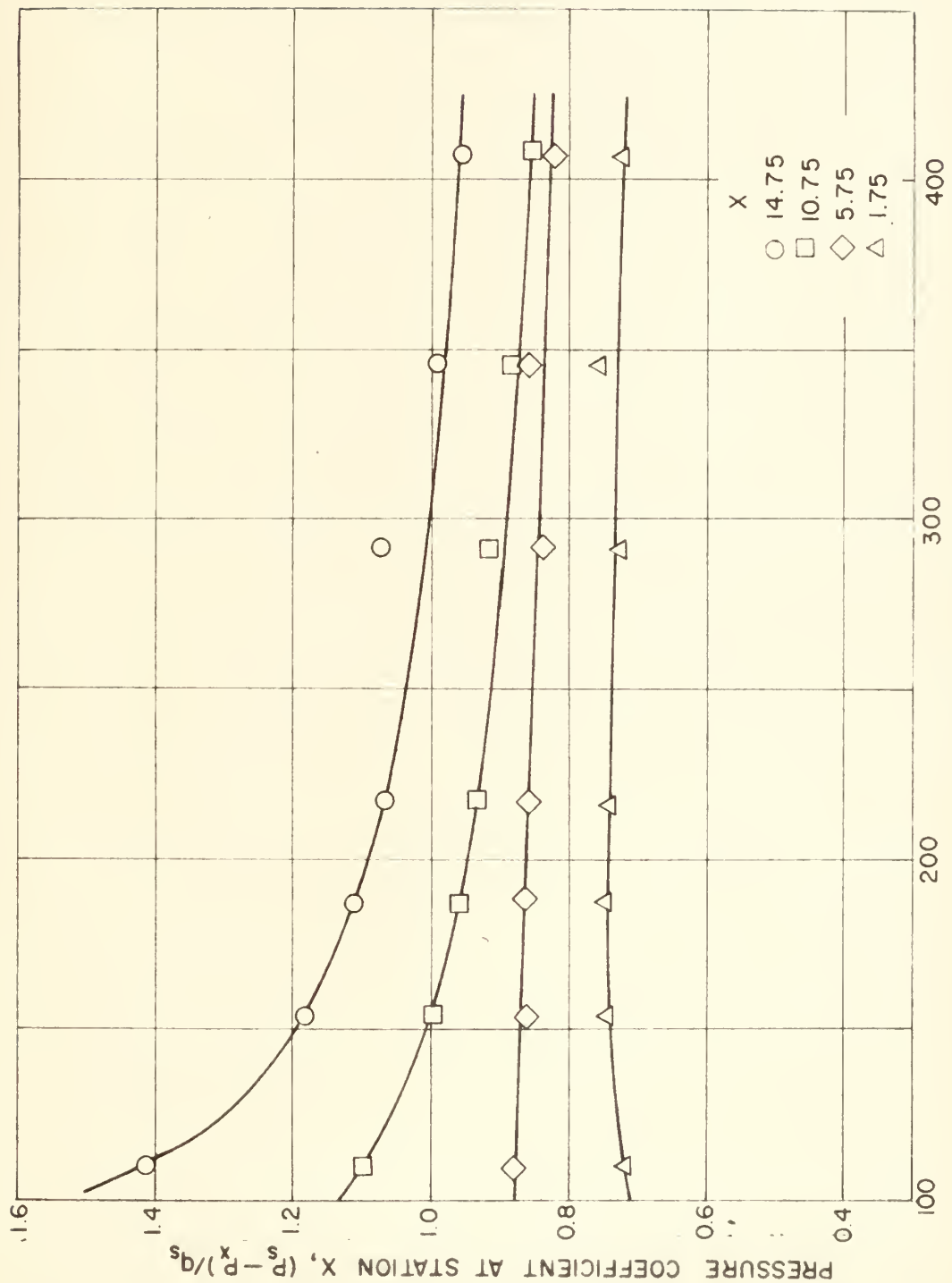

Figure 24. Pressure Coefficient Versus Mixture Velocity at Various Stations Downstream of Flameholder; $\phi = 1.0$, 1.0 inch Diameter Flameholder.

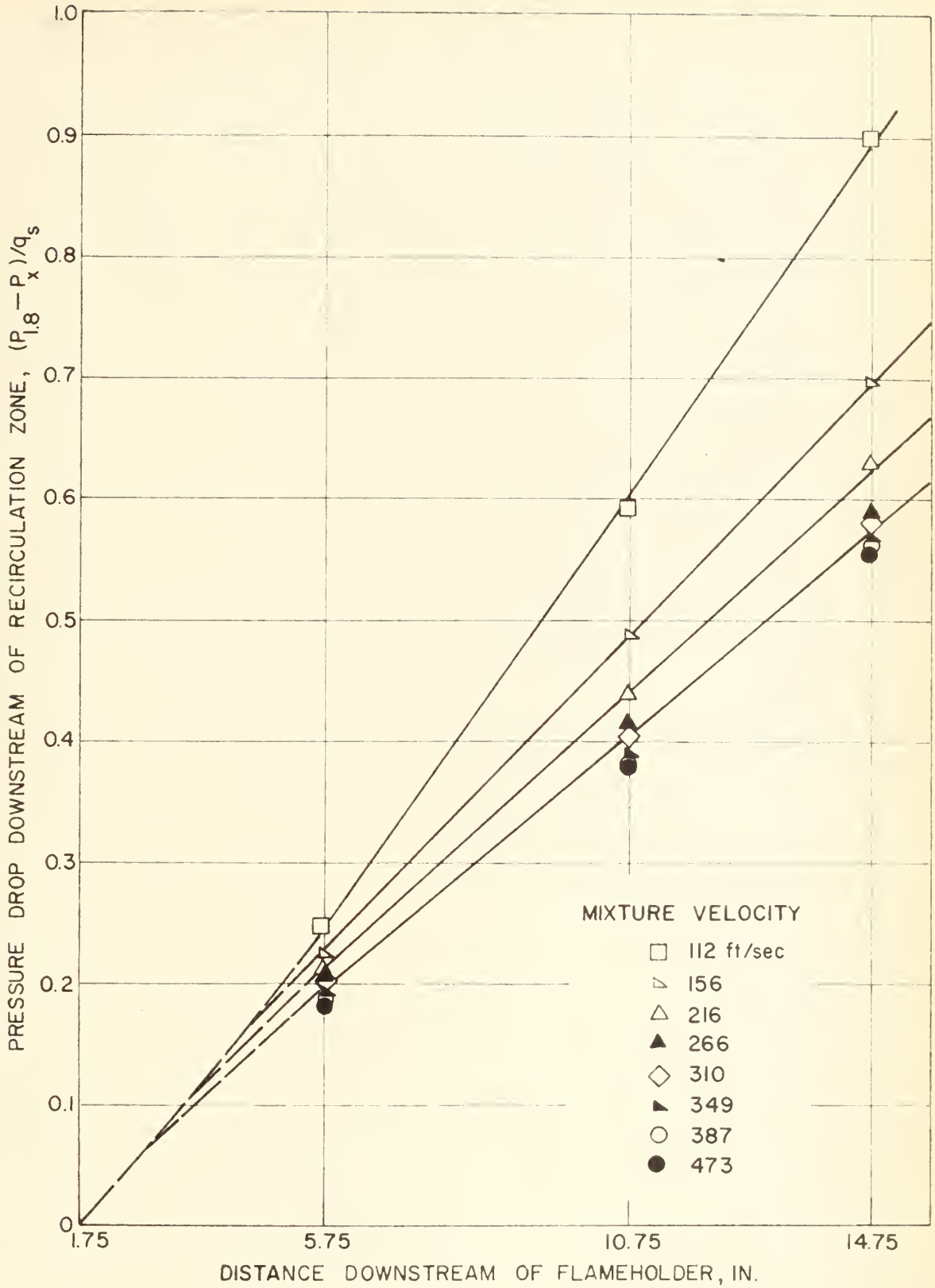

Figure 25. Pressure Drop Downstream of Recirculation Zone Versus Distance Downstream of Flameholder. ϕ = 1.0, 1/8 inch Diameter Flameholder

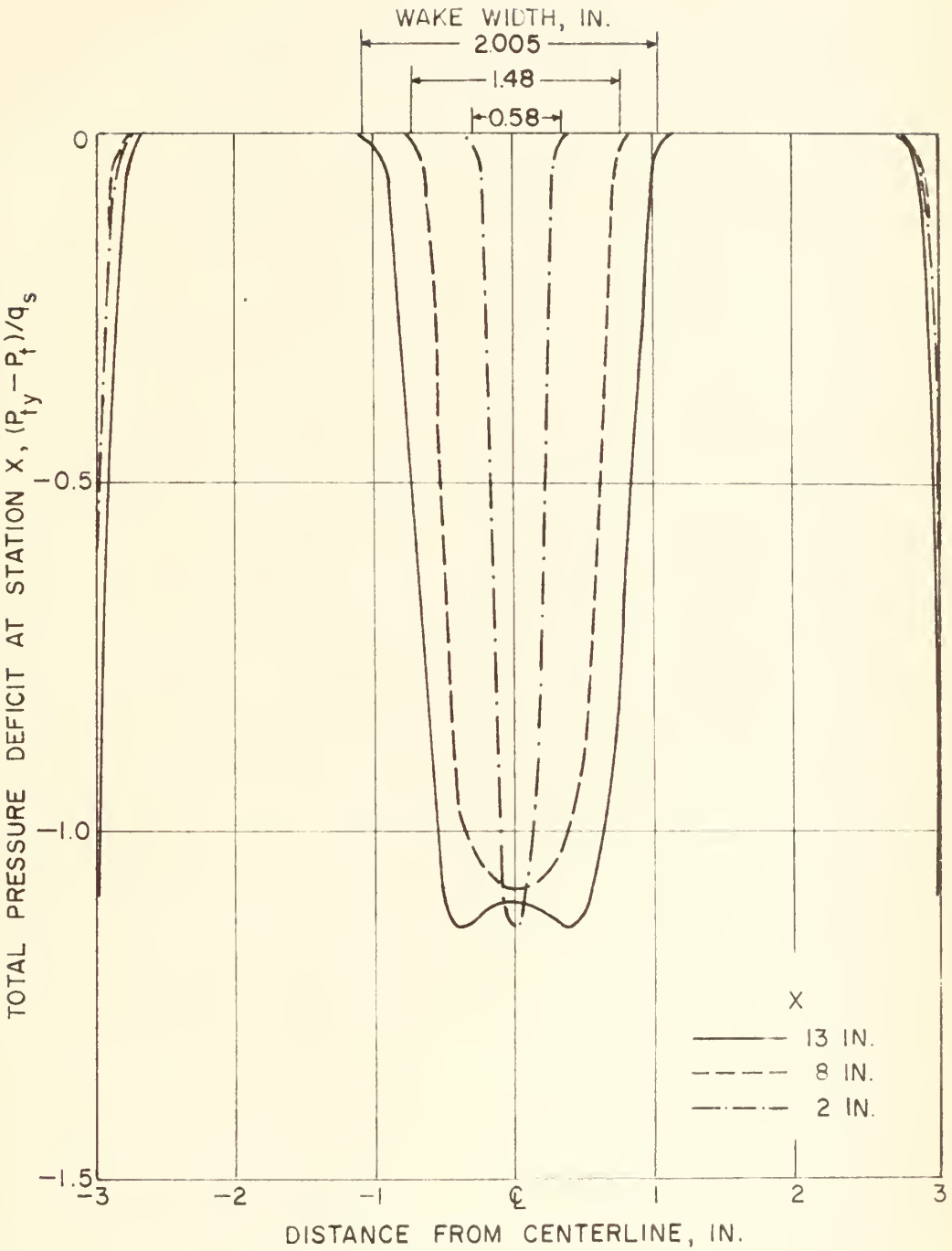

Figure 26. Total Pressure Deficit Across Duct Through Flame Stabilized by 1/8 inch Diameter Flameholder; ϕ = 1.0, 292 ft/sec Mixture Velocity.

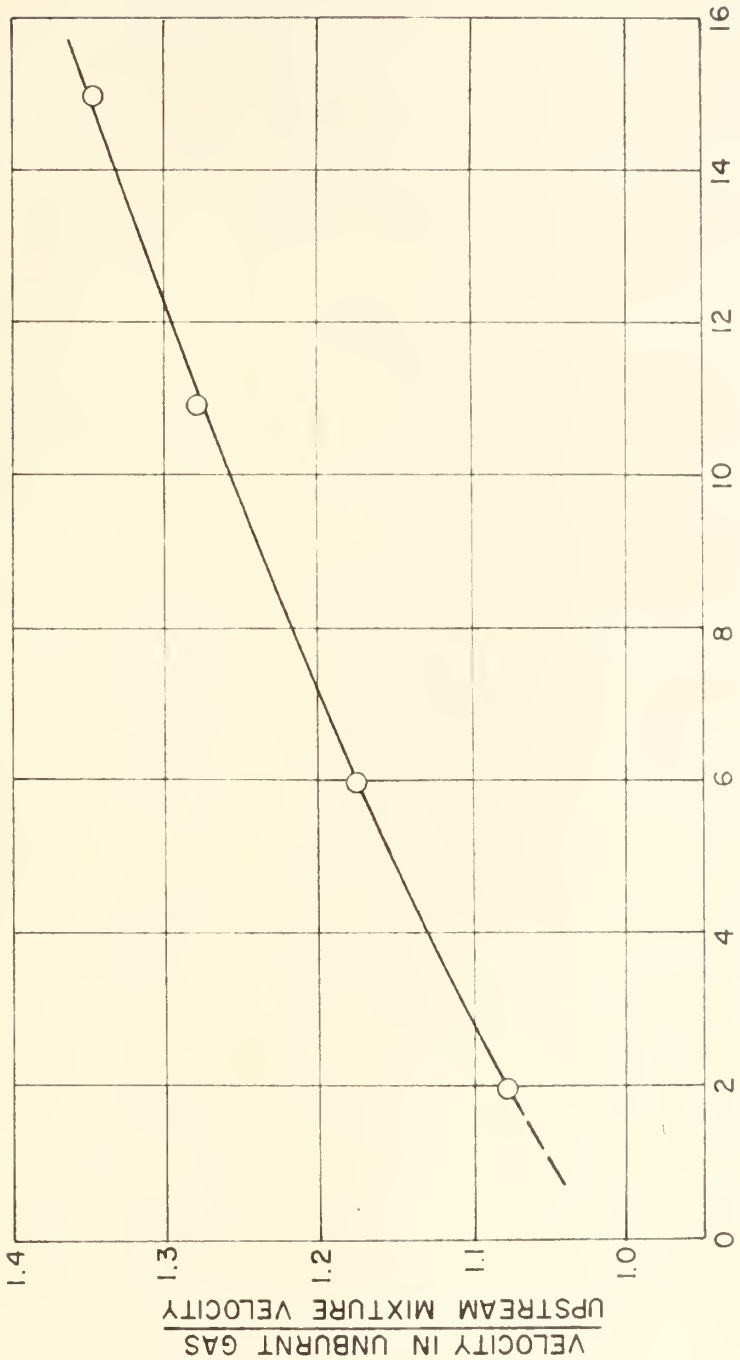

Figure 27. Normalized Unburnt Gas Velocity Versus Distance Downstream; ϕ = 1.0, 292 ft/sec Mixture Velocity, 1/8 inch Diameter Flameholder.

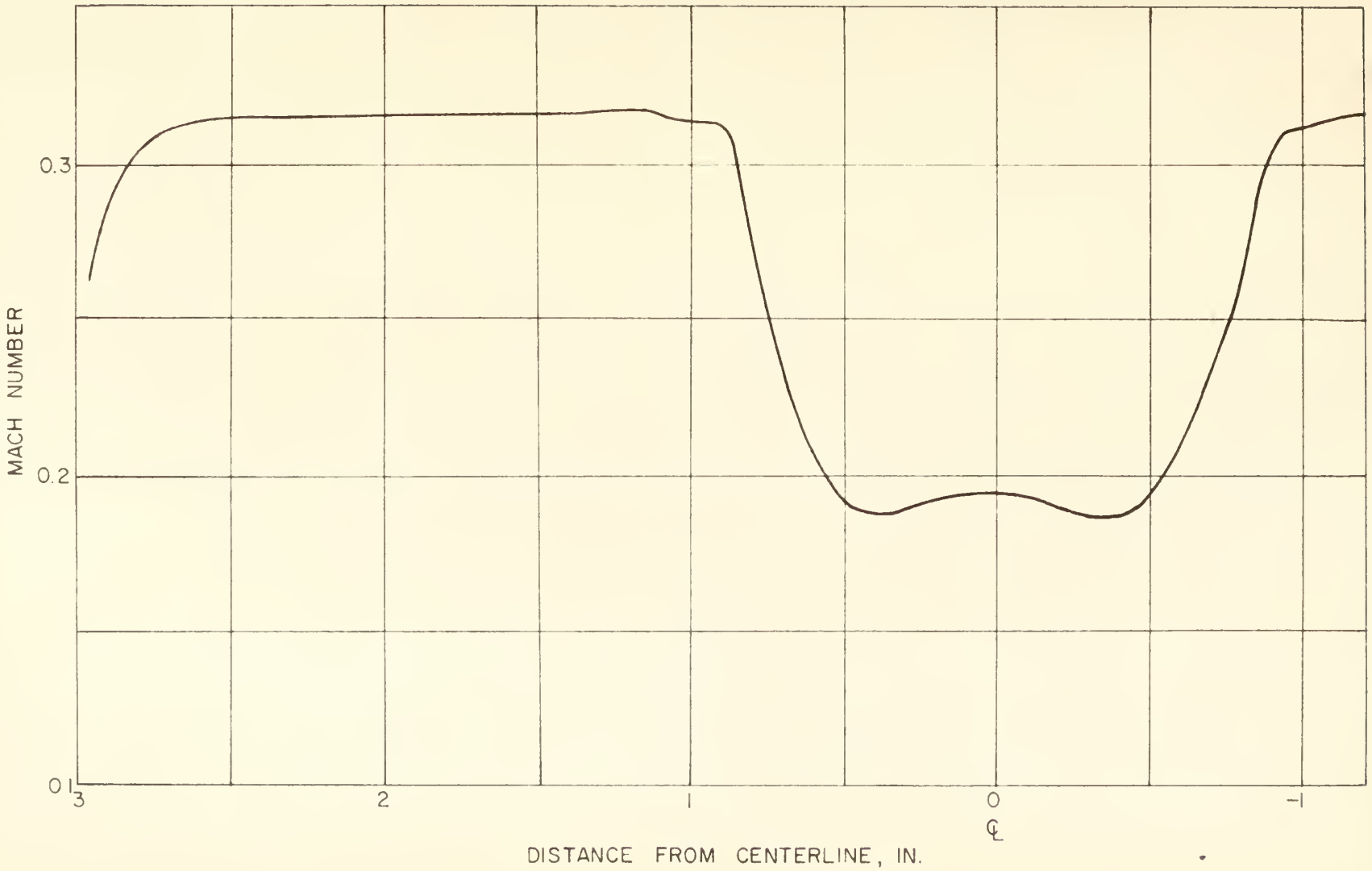

Figure 28. Mach Number Profile Across Duct at 14 inches Downstream of Flameholder; ϕ = 1.0, 292 ft/sec Mixture Velocity, 1/8 inch Diameter Flameholder.

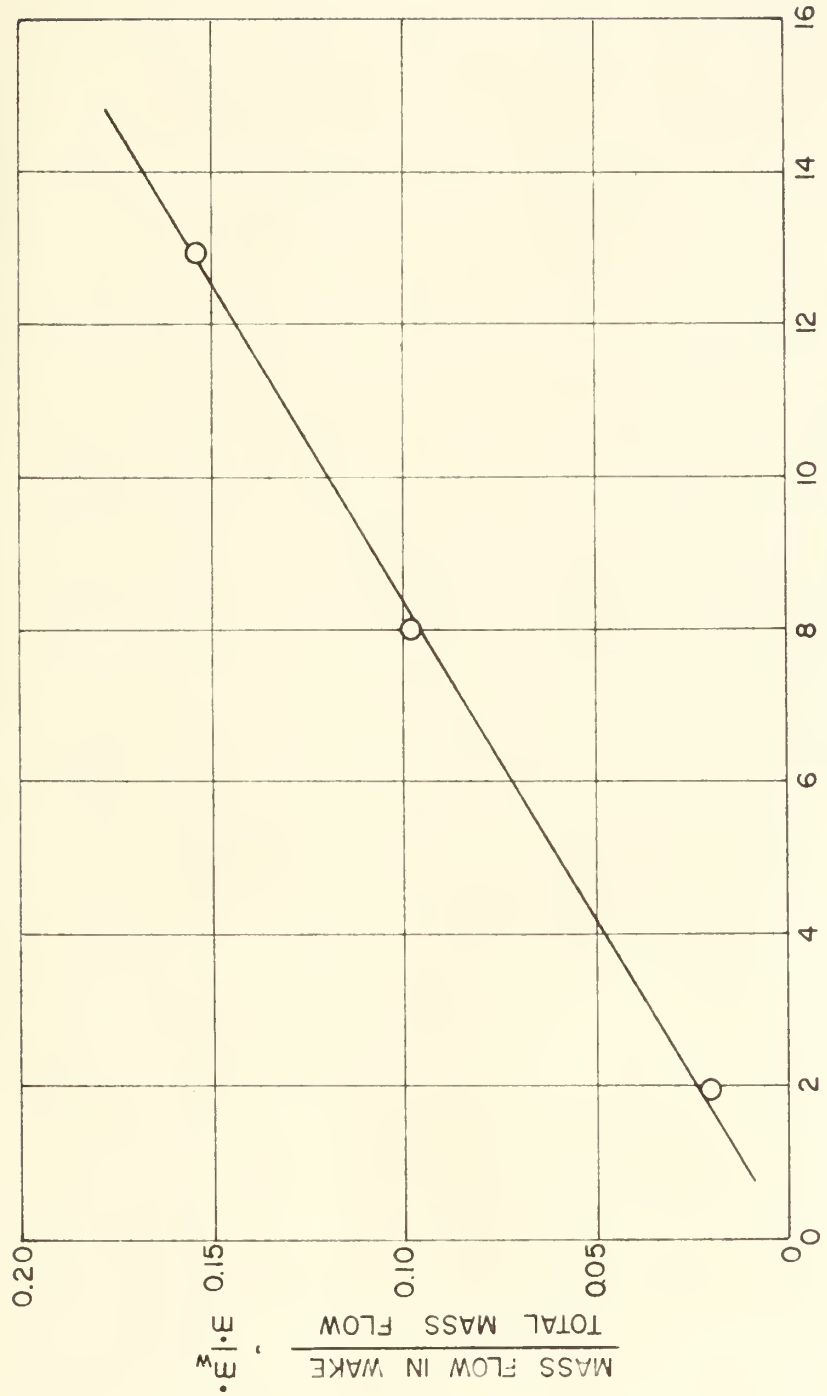

Figure 29. Fraction of Total Mass in Wake Versus Distance Downstream; $\phi = 1.0$, 292 ft/sec Mixture Velocity, 1/8 inch Diameter Flameholder.

thesT464
An experimental investigation of flame s
3 2768 002 03526 3
DUDLEY KNOX LIBRARY